T.R.
GEBZE TECHNICAL UNIVERSITY
GRADUATE SCHOOL OF NATURAL AND APPLIED SCIENCES

ACTIVE THERMAL MANAGEMENT OF A MILITARY COMPUTER WITH VAPOR COMPRESSION COOLING

SALİH CAN DÖNMEZ
A THESIS SUBMITTED FOR THE DEGREE OF
MASTER OF SCIENCE
DEPARTMENT OF MECHANICAL ENGINEERING

GEBZE
2019

T.R.

GEBZE TECHNICAL UNIVERSITY

GRADUATE SCHOOL OF NATURAL AND APPLIED SCIENCES

ACTIVE THERMAL MANAGEMENT OF A MILITARY COMPUTER WITH VAPOR COMPRESSION COOLING

SALİH CAN DÖNMEZ

A THESIS SUBMITTED FOR THE DEGREE OF

MASTER OF SCIENCE

DEPARTMENT OF MECHANICAL ENGINEERING

THESIS SUPERVISOR

ASSOC. PROF. DR. MUSTAFA FAZIL SERİNCAN

GEBZE

2019

T.C.
GEBZE TEKNİK ÜNİVERSİTESİ
FEN BİLİMLERİ ENSTİTÜSÜ

BUHAR SIKIŞTIRMALI SOĞUTMA İLE ASKERİ BİLGİSAYARIN AKTİF TERMAL YÖNETİMİ

SALİH CAN DÖNMEZ
YÜKSEK LİSANS TEZİ
MAKİNE MÜHENDİSLİĞİ ANABİLİM DALI

TEZ DANIŞMANI
DOÇ. DR. MUSTAFA FAZIL SERİNCAN

GEBZE
2019

GEBZE TEKNİK ÜNİVERSİTESİ	YÜKSEK LİSANS JÜRİ ONAY FORMU

GTÜ Fen Bilimleri Enstitüsü Yönetim Kurulu'nun 03/07/2019 tarih ve 2019/30 sayılı kararıyla oluşturulan jüri tarafından 29/07/2019 tarihinde tez savunma sınavı yapılan Salih Can Dönmez'in tez çalışması Makine Mühendisliği Anabilim Dalında YÜKSEK LİSANS tezi olarak kabul edilmiştir.

JÜRİ

ÜYE (TEZ DANIŞMANI)	: DOÇ. DR. MUSTAFA FAZIL SERİNCAN
ÜYE	: PROF. DR. FEVZİ BEDİR
ÜYE	: PROF. DR. BURAK DİKİCİ

ONAY

Gebze Teknik Üniversitesi Fen Bilimleri Enstitüsü Yönetim Kurulu'nun

...../...../..... tarih ve ...../..... sayılı kararı.

SUMMARY

In today's world, the people try to innovate and look for new technologies in order to make their life easier. When the people produce these things, they have to pay attention to the product's quality and capacity. This is because some significant effects such as working at high temperature, high pressure etc. can reduce their product's quality and its life.

In this study, the design and use of a mini scale refrigeration system will be offered instead conventional cooling methods for a computer used in military applications. It is aimed to design a novel system to improve the cooling of the military computer case.

Mini scale compression refrigeration system to be developed in this study comprises of a mini compressor, an expansion device, a condenser and evaporators.

Evaporator is a component that take heat from the heat source to increase temperature. The evaporator therefore should be designed to be in direct contact with the heat source. The pressure drops, the heat transfer coefficients, the inlet and outlet conditions will be taken into account, while selecting materials and determining evaporator and compressor capacity. The evaporator capacity and power of the compressor will be used to calculate the condenser capacity.

Keywords: Compression Refrigeration Cycle, Computer Cooling Application, Evaporator Design, Thermal Management.

ÖZET

Günümüzde insanlar yaşamlarını daha kolay yaşayabilmek amacıyla yenilik yapmaya ve yeni şeyler aramaya çalışmaktadır. İnsanlar bu yenilikleri üretirken ürünlerinin kalitesi ve kapasitesinin farkında olmaları gerekmektedir. Yüksek sıcaklık ve basınç gibi bazı etkiler ürünlerin kalitesini ve yaşamını etkilemektedir.

Bu çalışmada, askeri uygulamalar için kullanılan bilgisayarın soğutulması işleminde görev alan geleneksel soğutma yöntemlerinin yerine bilgisayara uygun tasarlanan mini ölçekli soğutma çevriminin kullanılması teklif edilmektedir.

Bu çalışma için geliştirilen mine ölçekli sıkıştırmalı soğutma çevrimi, mini kompresör, genleşme vanası, yoğuşturucu ve buharlaştırıcılardan oluşmaktadır. Buharlaştırıcı, ısı kaynağından ısı çekerek sıcaklığın düşmesini sağlayan bir bileşendir.

Buharlaştırıcının ısıl kaynak ile direkt temas ettirilmesi sağlanarak dizaynı yapılmalıdır. Malzeme seçimi yapılırken ayrıca buharlaştırıcı ve kompresör kapasitesi belirlenirken; basınç düşümü, ısı transfer katsayısı, giriş ve çıkıştaki koşullar göz önüne alınmalıdır. Buharlaştırıcı kapasitesi ve kompresör gücü, yoğuşturucu kapasitesi hesaplamakta kullanılmaktadır.

Anahtar Kelimeler: Bilgisayar Soğutma Uygulamaları, Buharlaştırıcı Tasarımı, Sıkıştırmalı Soğutma Çevrimi, Termal Yönetim

ACKNOWLEDGEMENTS

This research project was included within the scope of The Researcher Training Program for Defense Industry Project and was supported by ASELSAN.

I would first like to thank my thesis advisor Assoc. Prof. Mustafa Fazıl SERİNCAN for the continuous support, guidance and endless patience during this period of project.

Second, I thank to ASELSAN, especially Dr. Tolga KÖKTÜRK and Dr. Serkan KAYILI, for their valuable suggestions and helps. I also thank Fethiye KÜÇÜK for her collaborations during this research project, Halis KILIÇ and Fatih ÖNGÜL for their help to manufacture and integrate the cooling system components and computer case.

Very special thanks to my family and my friends, I could not do anything without them. Finally, I dedicate this project to my nephew Kuzey Kaan DÖNMEZ ,who is a new member of my family, and dedicating in memory of my grandfather.

TABLE of CONTENTS

LIST of ABBREVIATIONS and ACRONYMS

Abbreviations and Acronyms	**Explanations**
μ	: Dynamic Viscosity
η	: Isentropic Efficient
Ω	: Omega
ΔP_{acc}	: Acceleration Pressure Drop
ΔP_{single}	: Single-Phase Pressure Drop
ΔP_{tp}	: Two-Phase Pressure Drop
A	: Area
Bo	: Boiling Number
Co	: Convection Number
C	: Celsius
COP	: Coefficient of Performance
CFD	: Computational Fluid Dynamics
D	: Diameter
dBA	: Decibel
EES	: Engineering Equation Solver
evap	: Evaporator
F	: Fahrenheit
f	: Friction Factor
F_{fl}	: Surface Parameter
FFF	: Fanning Friction Factor
Fr	: Froude Number
g	: Gram
h	: Enthalpy
h_{tp}	: Two Phase Heat Transfer Coefficient
h_{lo}	: Single Phase Heat Transfer Coefficient
K	: Kelvin
kPa	: Kilopascal
m	: Meter
mm	: Millimeter

MPa	:	Megapascal
$\dot{m}$	:	Mass Flow Rate
liq	:	Liquid
lo	:	Liquid Only
lv	:	Liquid-Vapor Mixture
Nu	:	Nusselt Number
Pa	:	Pascal
Pr	:	Prandtl Number
P&ID	:	Piping and Instrumentation Diagram
Re	:	Reynolds Number
RPM	:	Rotation per Minute
$Q_{coo.cap}$	:	Cooling Capacity
s	:	Entropy
T_m	:	Refrigerant Temperature in the Evaporator
tp	:	Two-Phase
T_s	:	Wall Temperature
T1	:	Channel Temperature
W	:	Watt
W_c	:	Compressor Power
x	:	Refrigerant Quality
vap	:	Vapor

LIST of FIGURES

LIST of TABLES

1. INTRODUCTION

1.1. General Information

In today's modern world, technological tools have become a necessity for human life. Especially, computers are used in many areas of people's life. For this reason, people expect to use them without any problem. The computers can reach high temperatures while working, thus the most common problems occur in computer which are the overheating and removal of this heat. Different types of cooling methods are used in order to decrease this temperature.

Air cooling system is the easiest method to control the operating temperature of electronic devices. Air gives an opportunity to increase natural and forced convection effects on computer electronics. However, it cannot be used under high ambient temperature condition. In other words, operating conditions cause to design a new cooling method instead of conventional cooling methods.

In this thesis, new cooling methods has been studied as an alternative to air then the novel compression refrigeration cycle design develops for the computer which is used in military applications. Military computers have to be designed and constructed according to Military Standards and Specifications (MIL). They are much more robust than other types of computers and they can work accurately under intended environmental conditions such as extreme temperature, limited humidity range etc. When they are considered as main elements, the compression refrigeration cycle usually supplies enough capacity to operate these conditions. As a result of this cycle, the optimal cooling design is obtained thanks to modeling and experimental analysis.

Two main programs are used in this thesis: The first one is Engineering Equation Solver (EES) to find out thermodynamic properties of the refrigeration cycle. Matlab is the second one to size the evaporator channels and define the evaporator. properties such as pressure drops and heat transfer coefficients.

In the final part of the thesis, the computer test bench is produced according to dimension values which are obtained from Matlab. Hence, it can be possible to make comparison between the mathematical model and experimental data.

1.2. Basics of Vapor Compression Refrigeration Cycle

In the technology age, the cooling system design plays an important role in the maintenance of the performance. The cooling system can manage the temperature degree of the system by the help of refrigerant. The vapor compression refrigeration cycle is described as the most commonly used method to build a high performance cooling system.

Vapor compression refrigeration cycle is used to transfer a great amount of heat energy among the hot reservoir, cold reservoir and refrigerant. The hot reservoir is defined as ambient temperature and the cooling place temperature also is called cold reservoir. There is an interaction between reservoirs and heat transfers from hot reservoir to cold one. The heat transfer relation between the reservoirs is shown in Figure 1.1.

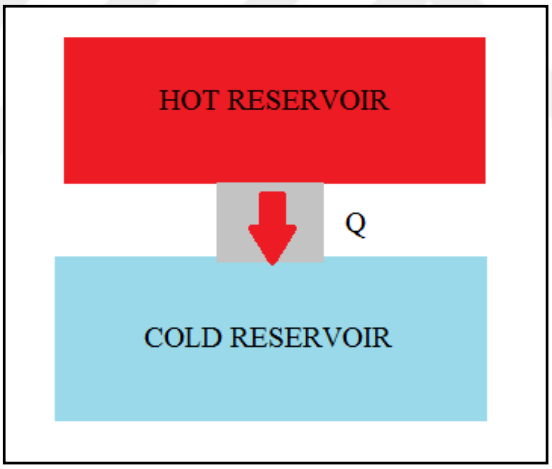

Figure 1.1: Heat Transfer Between Reservoirs.

This basic cycle usually consists of four main components: evaporator, compressor, condenser and expansion valve. Each component in the system has its own role to determine and regulate the pressure and temperature values of the system. In addition, all components are connected by the piping system [1]. Figure 1.2 shows the main components and the connection of them along the system.

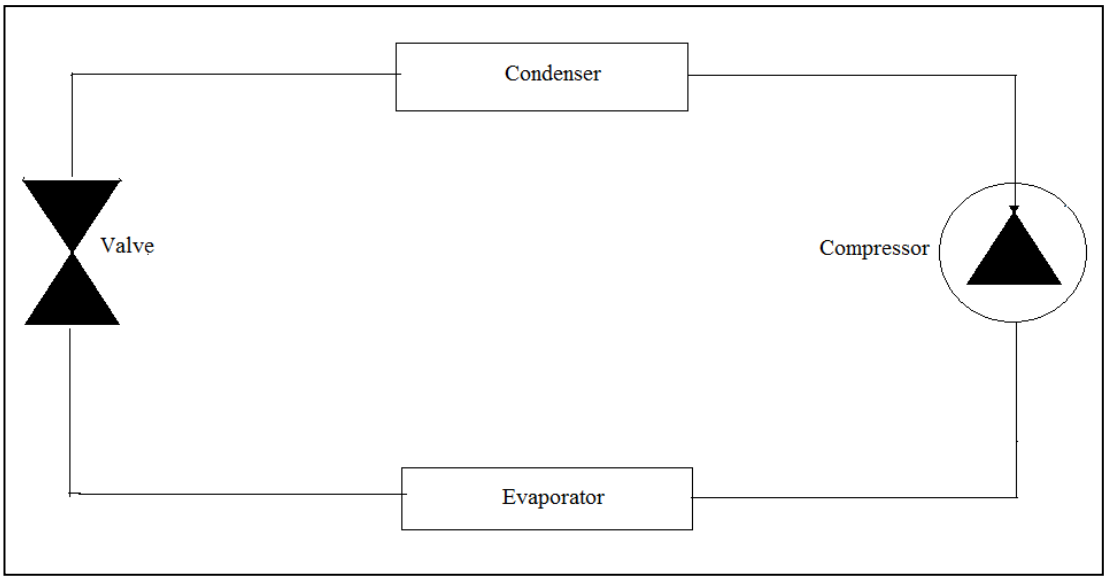

Figure 1.2: Compression Refrigeration Cycle Components.

Ideal vapor compression refrigeration cycle is the most used method for refrigerant systems. Table 1.1. shows the working principle of this cycle at specific ranges.

Table 1.1: Working Principle of Refrigeration Cycle.

1-2	Isentropic compression process in the compressor
2-3	Heat transfer at constant pressure from the condenser to the ambient
3-4	Pressure drop by using the expansion valve
4-1	Heat transfer at constant pressure from the evaporator to the refrigerant

In this cycle, the refrigerant enters the compressor as saturated vapor and it is compressed isentropic to the condensing pressure. During the compression process, the refrigerant temperature becomes higher than the ambient temperature. The refrigerant then enters the condenser as superheat vapor and leaves the condenser as saturated liquid. The refrigerant temperature is still higher than the ambient.

The saturated liquid refrigerant flows through the expansion valve to decrease its pressure to the evaporator pressure. The refrigerant which leaves the expansion valve turns from the saturated liquid into the liquid-vapor mixture and its

temperature also becomes lower than the environment where the evaporator is placed. After that, it enters to the evaporator with low quality and take heat from the environment to be cooled. Finally, it comes back to compressor as a saturated vapor and this cycle completes its mission [2].

There are two kinds of diagram in the vapor compression cooling cycle. Temperature - entropy diagram is usually used to determine energy transfer in the system. This diagram also shows the cycle points and the curve of pressure which is shown as a red curve in Figure 1.3. The area under this curve symbolizes the heat transfer between among components, refrigerant and ambient air.

Another diagram is composed by the relationship between refrigerant pressure and enthalpy values of the whole system. The curve in the P-h diagram describes the temperature distribution of the refrigerant.

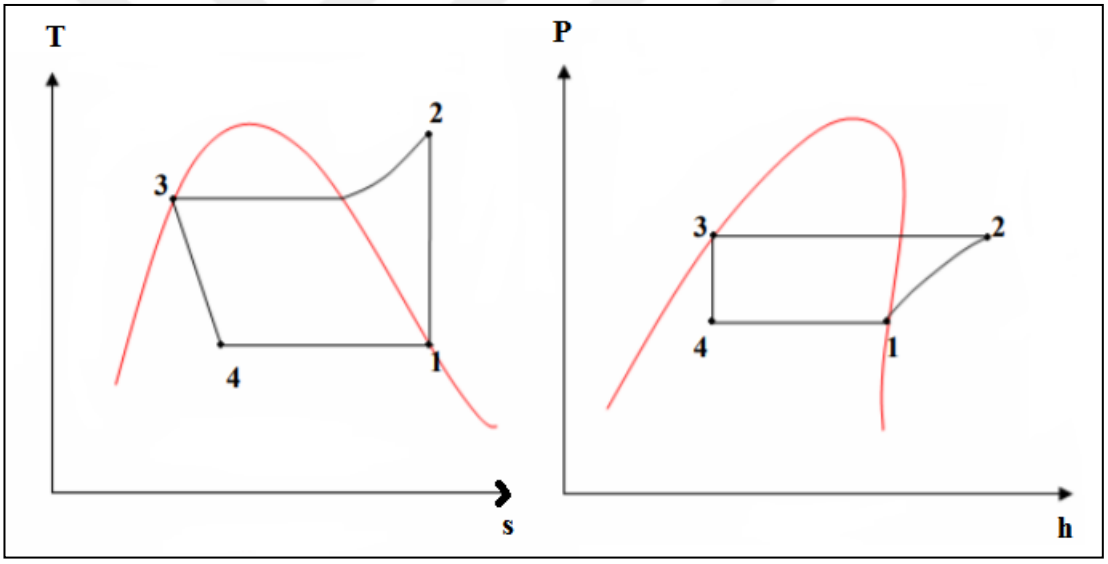

Figure 1.3: T-s and P-h Diagrams of Vapor Compression Refrigeration Cycle.

1.3. The Methodology of Study

The analysis studies of the development of the refrigeration system for military computer application are explained step by step below:

- To analyze the optimum side wall temperature when the computer runs at full power.
- To determine the cooling capacity in compliance with safety standards.

- To investigate the refrigeration system components and the proper refrigerant type with limitations of this study.
- To select the compressor depending on the limitations and determine the evaporator and condenser temperature due to its properties such as operating temperature, maximum operating pressure etc.
- To determine the effect of changing the evaporator temperature on the cooling cycle and also finding different temperature values to create an alternative for the cooling system.
- To solve the ideal compression refrigeration equations under different evaporator temperature conditions by Engineering Equation Solver in order to find and store the thermodynamic properties of R134a.
- To convey the results of thermodynamic properties to Matlab and obtain the heat transfer coefficient and temperature difference values for preliminary design of the evaporator.
- To change the dimension of evaporator in order to find the optimum pressure drop and heat transfer coefficient of the cycle, also temperature distribution of the side walls.
- To build the test bench to study experimentally and make comparison between the mathematical and experimental data.

1.4. Literature Review for Design of Refrigeration Cycle

The literature on design of refrigeration cycle has highlighted several important topics and circumstances to build a novel system. The various studies from literature are given in this section.

One of the first studies on the complete cycle is conducted by Heydari [3]. This study is about designing a new cycle which called a miniature CPU cooling system. The components of CPU cooling system are designed by mathematical formulations and also modeled according to parameters such as working refrigerant, evaporating and condensing temperatures, overall efficiency of system etc. In addition, the effects of variation of evaporating, condensing temperature and choice of refrigerant on COP of system is shown by diagrams.

Chang et al. [4] analyze the thermal performance of the miniature refrigeration system for electronic cooling. Four main components are experimentally investigated with using R-134a as a refrigerant. The opening expansion valve numbers and input heating power are changed respectively, then the largest cooling capacity of system, 150 Watt, is obtained from experimental studies. Additionally, they find the input heating power and the expansion valve which is opened respectively have a major effect on the performance of the refrigeration system.

Yildiz [5] examines to design the compression refrigeration cycle for a miniature refrigeration system. The purpose of this project is to develop a code for the components of refrigeration system and try to find an alternative solution for the cooling problems. This code is developed by Matlab and used for the simulations. The cold space temperature, ambient temperature, evaporation and condensation temperatures are considered as design parameters.

The study of Trutassanawin et al. [6] demonstrates that the numerical analysis of a miniature refrigeration system for cooling the electronic chip. A system model code which is written in Matlab investigates the inlet and outlet conditions of refrigerant through the four components and piping system at around different temperature range. In addition, experiments are conducted to compare results with model, which is obtained by Ansys Fluent software.

Mongia et al. [7] research the design of the miniature refrigeration cycle for the computer which has 50 Watt of heat capacity. This system includes the cold plate compressor, condenser and expansion valve with iso-butane as the refrigerant. After the system is built, it is tested with mathematical data in order to determine overall system performance.

According to Mehendale et al. [8], the system heat transfer coefficients are based on the inlet and the outlet refrigerant temperature and not the bulk temperature in all studies. Detailed examination of the single phase, two phase flow and heat transfer in channel with different geometries are made and their results are compared with the previous studies on this topic.

To determine the effects of two phase flow, Ide et al. [9] reports on the results of investigations into the characteristics of an air-water isothermal two-phase flow in mini-channels, in capillary tubes with inner diameters of 1 mm, 2.4 turn, and 4.9 mm respectively.

Another important topic is the determination of the heat transfer coefficient and pressure drop parameters in the evaporator. One study by Hsieh and Lin [10] examine the vertical heat exchanger for refrigerant R-140A. Experiments are conducted in this study in order to calculate the heat transfer coefficient and pressure drop at different operating conditions. The mass flux of refrigerant in the channel is changed from 50 to 100 kg/m^3, also the vapor quality from 0.20 to 0.80. Additionally, the system pressure fixes at 1.08 and 1.25 MPa.

Lazarek et al. [11] study the refrigerant R-113 in a round channel tube to measure the heat flux, heat transfer coefficient and pressure drop. The measurement approach is based on single- and two-phase flow methods. The measurements are calculated with using a round tube with an internal dimension of 3.1 mm and lengths of 123 and 246 mm.

Kandlikar and Steinke [12] investigate the flow boiling process in the micro- and mini-channels with different shapes and geometries to refrigerate the electronic devices, fuel cells and other applications. As a result of this study, they have found that the single-phase liquid flow is generally in the laminar region in mini-channels and micro-channels. The transition between the laminar and turbulent flow is discussed considering the single-phase liquid flow. However, it cannot be well defined in this study.

Surveys such as that conducted by Signal et al. [13] analyze the pressure drop in a single and two phase flow. Three types of pressure drop occur in refrigerant: Frictional, acceleration and gravitational. They are investigated in this study with managing different proper pipe material, fittings and valves.

A miniature compressor has a unique role to build the compression refrigeration system for the electronics cooling applications. Studies such as that conducted by Sathe et al. [14] have investigated the working performance of the miniature compressors. In this paper, the performance measurement on the miniature compressor with R-134a as the refrigerant is researched. Each test is conducted by varying pressures and rotational speeds at the superheat of 5 K in order to calculate the refrigerant mass flow rate, power consumption and temperature distribution.

Coskun [15] examines the relationship of working on high the ambient temperature and its effect to the computer cabin walls. In her study, a new approach has been developed under two phase flow condition and it is performed with

computational fluid dynamics analysis. In her CFD analysis, refrigerant quality changes from 0 to 0.70-0.80 along the length of evaporator channel and the unstable heat flux is used as an initial condition.

My master thesis and her thesis are based on and related to the same issue that the novel cooling system design to allow people working at high ambient temperature. For this purpose, Coskun investigates the two-phase flow method using CFD to find out the optimum thermal distribution. Her findings also demonstrate that the changing of the quality along the pipe length is observed increasing cumulatively and this increase is not linear.

In my thesis, I focus on getting thermodynamic properties and transmitting them to make a parametric analysis for evaporator channel dimensions. When making comparison between her studies, my thesis assumes that the wall temperature fluctuations under the constant heat flux boundary conditions. Addition to this, the starting point of refrigerant quality is accepted according to thermodynamic properties result and the changing of this quality is assumed as linear along the evaporator channel length. Therefore, written Matlab code for this study can be used like a simple and smart evaporator design tool.

2. PRELIMINARY STUDY ON DESIGNING A NOVEL REFRIGERATION CYCLE

2.1. Algorithm of Study

The comprehensive study steps on thermal management of a military computer can be described as follows:

- The military computer has to be operated at 55^{o}C of ambient temperature. Side walls temperature should be decreased below 70 ^{o}C.
- Computer consists of nine power cards which have different heat loads and sum of them equals to 360 W. Therefore, the cooling capacity of this system is 360 W.
- Additional limitations such as computer dimensions and weight, economic conditions etc. are determined until selection of compressor and refrigerant.
- Compressor selection has a key role to build the cooling system. Moreover, refrigerant which can be used for selected compressor has to match the system conditions and limitations.
- Evaporating temperature should be calculated parametrically to create alternative cases for comparison.
- Thermodynamic properties in vapor compression refrigeration cycle can be obtained for four critical points using by Engineering Equation Solver according to ideal equations and selected compressor data.
- EES analysis is conducted for two different cases, then parameters such as mass flow rate, quality etc. transmit to Matlab software as input values.
- Matlab should be used for attaining both heat transfer coefficients and pressure drops of evaporator, as well as the temperature relation along the evaporator region between side wall, channel and refrigerant.
- Defining the pipe diameter for the evaporator channel.
- Evaporator is examined in two different zones according to the quantity of liquid and gas: Two Phase and Single Phase.
- Reynolds number for liquid and gas have to be found separately in two phase flow regions.
- Fanning Friction Factor should be calculated depending on Reynolds Number.

- Three types of pressure drop occurs in two phase flow regions: Liquid, Vapor and Acceleration. They should be found in order to calculate the total pressure drop value.
- Dimensionless numbers such as Boiling (Bo), Convection (Co), Froude (Fr) etc. are defined in proper Reynolds Number range, thus liquid only heat transfer coefficient can be calculated.
- Two phase heat transfer coefficients can be calculated by the helps of Kandlikar Correlation.
- Next step occurs in single phase flow region. Reynolds number should be calculated, and it is called as Reynolds Number for Vapor.
- Fanning Friction Factor and Nusselt Number in proper Reynolds Number range should be calculated by using with Gnilinski Correlation.
- Single phase heat transfer coefficient and pressure drops are found with the parameters above.
- The resistances among side wall, copper channel and refrigerant are taken into account for calculation the temperature distribution of the side walls.
- Ending of the Matlab session, Test Bench Preparation have remained to obtain new data for this study.
- Proper components are chosen according to mathematical data on refrigeration system and they are located to the computer cabin.
- Creating Test Matrices to ensure the conditions and test every possibility for robust system design.
- Finally, the results on using test bench are examined and findings are shown in figures and tables.

2.2. Determine the Working Conditions and Limitations

This project has been tried to be designed by considering various parameters which are the operating conditions and working limitations.

First of all, the capacity and ability of the system to be designed must require supplying an efficient power to continue the working of refrigeration cycle at the ambient temperature of 63 ^{o}C. The cards in the computer also dissipate about 360 Watt heat to the side walls of the computer. For this reason, the new system should

respond this issue as part of its job. When the calculation of thermodynamic properties of the cycle, the cooling capacity should equal to this heat value.

Refrigeration cycle design should also consider the computer dimension due to using on the military computer. Large component needs a larger working area. However, computer space negatively impacts to work with large components such as evaporator and condenser. Due to space limitations, high capacity and large compressors cannot be used as well.

Another essential issue is weight problem in the computer. The components of refrigeration cycle that will be placed inside the computer ought to be lightweight in order not to obstruct the transportability.

The performance or speed of a CPU depends on many factors; however, CPU temperature is the most important factor among them. When the specifications of CPU can be investigated and checked, the absolute maximum temperature value is 60^{o}C for long periods. Operating in safe conditions, it have to be reduced about 45-50^{o}C. Ideal CPU temperature can be obtained from the cooling process.

Last issue which should be taken into consideration is the selection of refrigerant. The refrigerant is an essential constituent part as well as other components of refrigeration cycle. Correspondingly, refrigerant is both used for its thermodynamic properties to develop a code and during the experiments on the test bench. Additional information about the refrigerant will be given in a following chapter.

2.3. Compressor Selection

Compressor is a mechanical device which could regulate and increase the pressure of the refrigerant in itself. The compressor has a critical important to safely design and complete refrigeration cycle. Hence, the compressor should be chosen carefully in order to obtain desirable conditions and properties.

2.3.1. Selection Criteria

Compressor selection method is mostly prepared according to the design criteria. The most important criterion for this project is the operating temperature. The compressor operates in a certain temperature range. Especially, compressor is to endure the high ambient temperature to maintain reliable process performance in this study. Additionally, the cooling system can provide the sufficient cooling capacity with operating evaporator temperature, therefore the compressor's limit should allow evaporator operating temperature to be risen or dropped.

Another important criterion is the capacity of compressor, because the cooling capacity depends on not only evaporator interaction, but compressor power. The compressor capacity and power could be changed and managed by rotational speed of the compressor. Thus, they could be used in a wide range of their capacities.

The latest criterion depends on the general rules of computer which should be lightweight and not take much space. A lightweight gives an opportunity to easily transport and safely work for the computer.

Due to these criteria, Aspen Miniature Compressors are considered as the first and best candidate for this thesis [16]. They are tested for varying pressure ratios, suction pressures and rotational speeds. Each test is conducted by the recommended superheat for Aspen compressors is 5 K. After these tests, they are ideally suited for the cooling electronics and in numerous commercial appliance types where space and weight are important.

2.3.2. Compressor Properties

After the selection criteria have been applied, it can appear that Aspen 3.8 cc Twin Series Compressor supplies enough power density to other components of the refrigeration system. It can be used with different types of refrigerant such as R134a, R410a or R404a. The changing speed range allows controlling the system in order to obtain high cooling capacity.

This type of compressor can be used in a wide range temperature of evaporator which is between about -30~24°C. Similarly, it can operate at high condenser

temperature of 71°C. However, its maximum ambient temperature is not sufficient to the operating conditions of study (49 °C).

As shown in Figure 2.1, the dimensions of Twin Series are coherent with the case study [16].

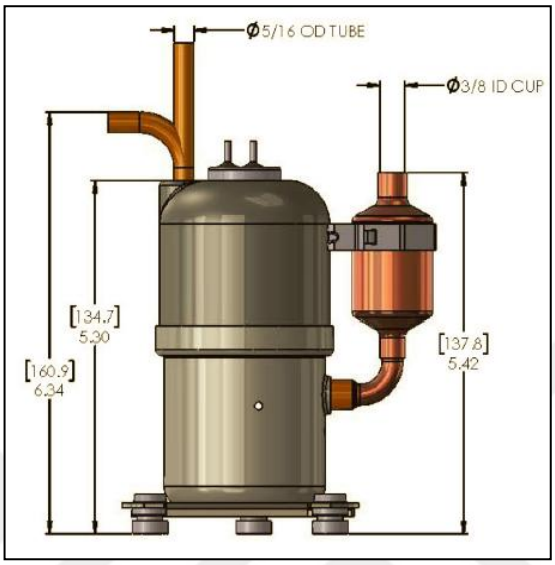

Figure 2.1: Dimensions of Twin Series Compressor.

The main properties of Twin Series Compressor are defined in Table 2.1.

Table 2.1: Main Properties of Aspen 3.8 cc Twin Series Compressor.

Compressor	3.8 cc Twin Series Low Noise, Miniature, Rotary BLDC Refrigeration Compressor
Refrigerant	R134a / R404a / R410a / R290a / R600a
Oil Type /Oil Quantity	Emkarate POE RL 68H / Factory Charged, 70 g
Speed Range	2100 – 6500 RPM
Evaporator Temperature Range	-30~24°C
Maximum Condenser Temperature	71°C
Maximum Ambient Temperature	49°C
Maximum Operating Pressure	2.4 MPa
Cooling Capacity	R-134a -ASHRAE T 3.8cc 910 W
Noise Level @ 1 meter	~ 40 dBA
Weight	~ 1800 g

Alternatively, Aspen Q Series compressor has equal properties with respect to the optimum operating temperature of Twin Series compressor. The disadvantage of this compressor is that its cooling capacity is less than Twin Series when both compressors are worked at low speed RPM. However, this value could provide sufficient energy at high speed for this thesis. Q Series compressor could be operated at 54^0C of maximum ambient temperature.

When it compares with the Twin Series which only can be worked at 49^0C, this condition provides the possibility to work with high temperature system. Additionally, its weight is approximately half of the Twin Series. Thus, it can be selected due to its light weight.

Figure 2.2 presents the dimension values of Q Series Compressor [16].

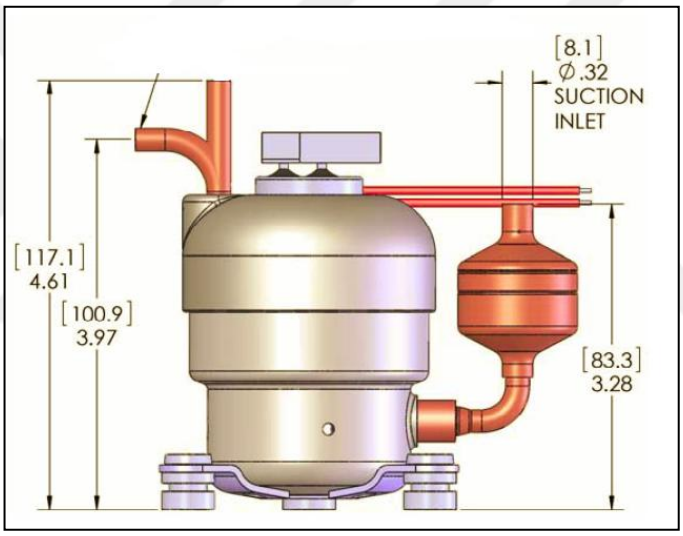

Figure 2.2: Dimensions and view of Q-Series Compressor.

Similarly, the properties of Q-Series could be seen from Table 2.2.

Table 2.2: Main Properties of Aspen Q-Series Compressor.

Compressor	Q-Series Low Noise, Miniature, Rotary BLDC Refrigeration Compressor
Refrigerant	R134a / R404a / R410a
Oil Type /Oil Quantity	Emkarate POE RL 68H / 23cc Factory Charged
Speed Range	2100 – 6500 RPM
Evaporator Temperature Range	-30~24°C
Maximum Condenser Temperature	71°C
Maximum Ambient Temperature	54°C
Maximum Operating Pressure	2.4 MPa
Cooling Capacity	R-134a -ASHRAE T 1.4cc 360 W -ASHRAE T 1.9cc 455 W
Noise Level @ 1 meter	~ 40 dBA
Weight	~ 900 g

Q Series compressor model has the high cooling capacity at high evaporating and condensing temperature and it is sufficient to be used in this thesis. When the condenser temperature is examined at evaporator temperature range of 10 to 20, it provides above the 360 Watt which is the cooling capacity required for the system.

The diagram of this data tested as Model T38 Rotary BLDC compressor from Aspen Compressor is demonstrated in Figure 2.3 [16].

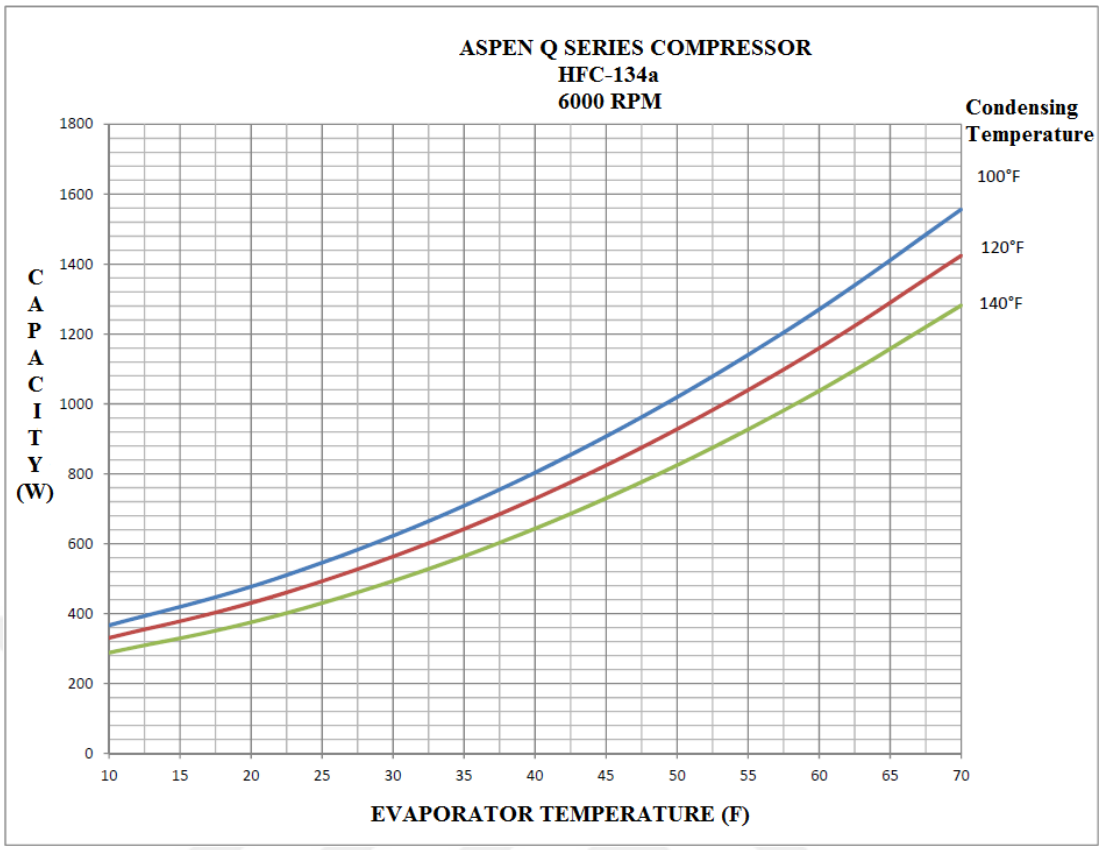

Figure 2.3: Aspen Q Series Compressor Capacity-Temperature Diagram.

Including the overall properties, both compressors comply with Military Standard Conditions which are accepted all over the world.

2.4. Refrigerant Selection

The selection of refrigerant is the most essential topic in order to obtain optimum performance and efficient from the cooling cycle, therefore it is needed to be selected carefully like the compressor, evaporator, condenser etc.

The various properties of the refrigerant should be taken into considered such as burning behavior, effect on global warming, its cost to design beneficial system at all points.

The global warming and pollution in the environment can be decreased by the careful selection of refrigerant. The refrigerant which contains the fluorine atom, causes the threat to the ozone layer, hence the most harmful refrigerants are R-11, R-12 and R-115. The desirable refrigerant also should be non-poisonous, inflammable.

Theoretical performance of the refrigerant previously can be predicted by analyzing the its thermophysical properties. Even though, every refrigerant has different thermodynamic properties when comparing with others, all of them have the same characteristic saturation curve. However, their phase change and critical point temperatures differ from other refrigerants.

The slope of the saturation curve increases as the selected refrigerant moves away from the critical point temperature. If the refrigeration cycle proceeds away from the critical point, this situation would become less vapor thanks to the pressure drop.

Above all, the refrigerant should be coherent with the selected compressor's standard. The miniature compressors which could be used in this thesis allows three types of refrigerant: R134a, R404a and R410a. Their thermodynamic properties are shown in Table 2.3. Refrigerants R410a and R404a have low critical point temperatures for operating system with the condenser temperatures of 70-75 °C on the contrary of using R134. [15].

Table 2.3: Some Critical Thermodynamic Properties of Refrigerants.

Refrigerant	Molar Weight (kg/Kmol)	Boiling Temperature at 1 atm (^{o}C)	Critical Point Temperature (^{o}C)
R134a	102.03	-26.1	101.1
R404a	97.60	-46.5	72.1
R410a	72.56	-50.5	72.5

Due to these reasons, the most suitable refrigerant is R134a and its pressure-enthalpy diagram presents the critical point in Figure 2.4.

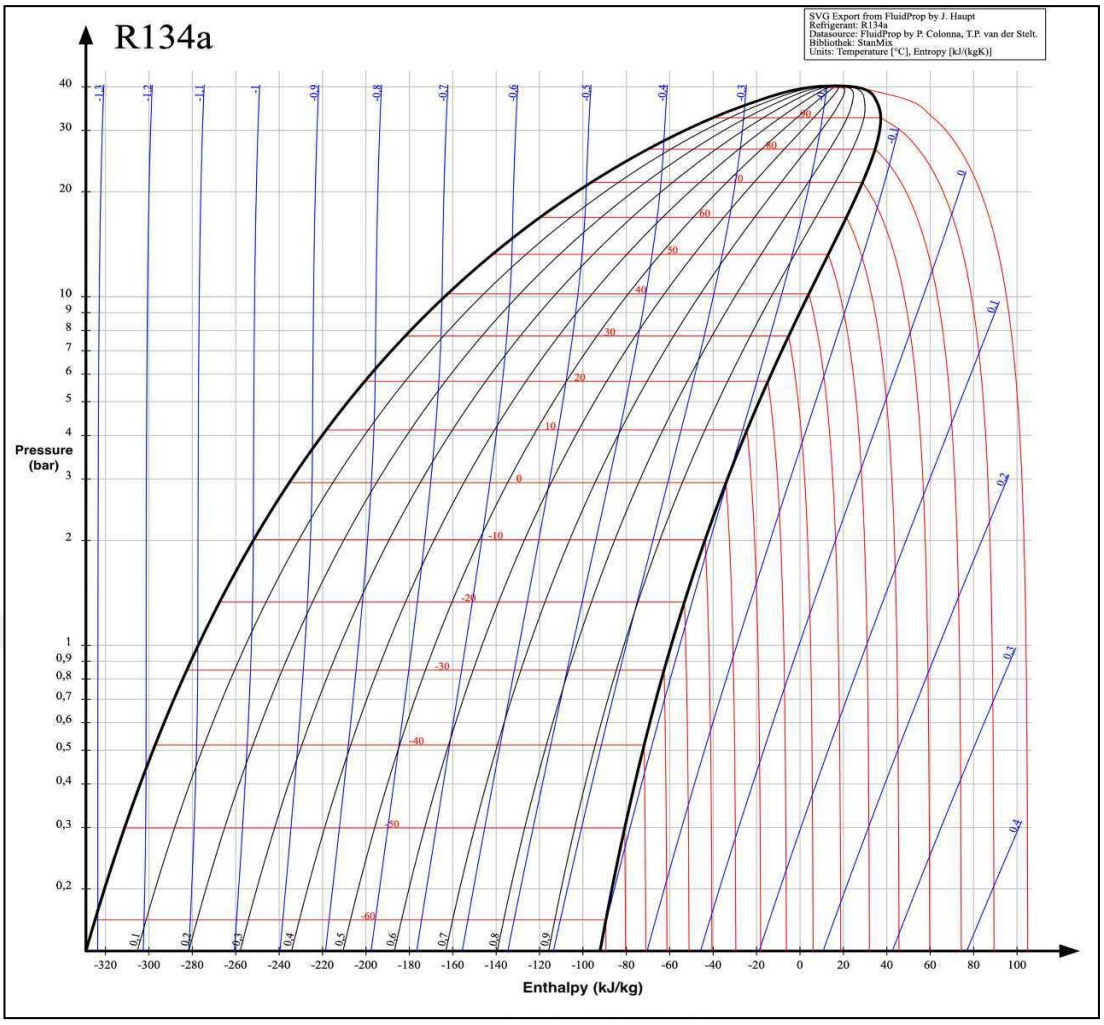

Figure 2.4: Pressure - Enthalpy Diagram of R-134a.

2.5. Analysis of Thermodynamic Refrigeration Cycle

2.5.1. Determination of The Initial Values

After the selection of refrigerant for this study, the thermodynamic properties of refrigeration cycle need to be calculated in order to effectively design the cooling system. The main purpose of this step is to determine the connection of the components of the cooling cycle and ensure the coordination between them.

The cooling cycle is based on equations and operating limitations. However, the cycle needs to be given values as initial conditions to the system in order to obtain thermodynamic properties of the system.

The compressor properties could be used as first initial conditions. The selected compressor has 2400 kPa of maximum operating pressure value. The maximum condensing temperature which is also an important property of compressor, could give an opportunity to be operated at 71 °C.

On the other hand, the compressor producing companies need to change the its temperature with superheat and subcool method, thus they could be reliably measured the cooling capacity of components. This compressor could allow 8 F of superheat (approximately 4.44 °C) and 10 F of subcooling (approximately 5.55 °C) in their application.

These properties have a strong connection between each other, thus condenser temperature could be calculated by using these values. The cooling capacity of cycle decreases when the condenser temperature is below 70 °C and the operating pressure is not higher than 2000 kPa. The condenser temperature should be higher than the ambient temperature, the operating pressure should also be lower than compressor operating pressure to reach the maximum cooling capacity.

The determination of the evaporator temperature depends on different parameters such as the condenser temperature, the compressor cooling capacity by changing its rotational speed.

Table 2.4 shows the values of relation between the temperature and pressure of R-134a from the pressure-enthalpy diagram. The critical temperature indicates the temperature value corresponding to the specified pressure value.

Table 2.4: Critical Pressure and Temperature Values of R-134a.

Pressure (kPa)	Critical Temperature (^{o}C)	Explanation
1963	66,62	The temperature and pressure values due to the subcooling process
2166	71	The most optimum relation between temperature and pressure for condenser
2400	75,66	Maximum operating conditions of the compressor

Calculation of compressor data in this study have at 71°C of condenser temperature by polynomial interpolation between different rotational speeds. Table 2.5 demonstrates the changes of the compressor cooling capacity with different temperatures and rotational speeds. The selected compressor provides the required cooling capacity at 4238 RPM at 10 °C of evaporator temperature. When this study is repeated at 20 °C of evaporator temperature, 500 W of cooling capacity which is needed, can be obtained at 2463 RPM.

Table 2.5: The Cooling Capacity of Selected Compressor (Q Series).

Condenser Temperature 160 F~ 71°C	Q_{in} Compressor Cooling Capacity (WATT)		
RPM	Evaporator Temperature 50 F~10°C	Evaporator Temperature 60 F~15.5°C	Evaporator Temperature 70 F~20°C
3000	316	458	594
4000	470	632	775
5000	613	784	956
6000	703	916	1131
	Qin=0.1304RPM-52.6		Q_{in} = 0.1792RPM + 58.4

As for the calculating of the compressor input power, it could be determined with using the obtained rotational speed values from the previous paragraph. Table 2.6 presents the compressor input power between 3000 to 6000 RPM.

Table 2.6: Compressor Input Power of Selected Compressor (Q Series).

Condenser Temperature 160 F~ 71°C	W_c Compressor Input Power (WATT)		
RPM	Evaporator Temperature 50 F~10°C	Evaporator Temperature 60 F~15.5°C	Evaporator Temperature 70 F~20°C
3000	242	252	261
4000	308	326	341
5000	372	397	418
6000	462	479	495

2.5.2. Determination of Equations

In this thesis, Engineering Equation Solver (EES) is used as a critical software in order to obtain the thermodynamic properties of the refrigerant system components. Hence, the cooling cycle equations should be carefully selected and transferred to this software.

This study finds the thermodynamic properties of refrigerant with using ideal vapor compression refrigeration cycle assumption. This assumption agrees with the law of conservation of energy as its main principle. The law of conservation of energy supports the idea that the energy cannot be created or destroyed, only transformed.

Similarly, mini compression refrigeration system components are presented as a model developed by Fischer [17]. The model that specify a heat exchanger model for the condenser and evaporator are explained by following equations.

2.5.2.1. Condenser Model

Analytical model of the condenser is based on three regions: Desuperheated, two-phase and subcooled. The initial properties of refrigerant in the condenser can be shown as T_{in}, P_{in} and $\dot{m}_r$. They are defined as the inlet temperature, pressure and

mass flow rate respectively. When refrigerant leaves from the desuperheated region, its thermodynamic properties turn into saturated vapor conditions and temperature and pressure values are symbolized by T_g and P_g, respectively. Heat transfer between each region can be described as:

$$Q_{dsh} = F_{dsh} L U_{dsh} \left(T_{c,dsh} - T_{c,air}\right) \tag{2.1}$$

$$Q_{tp} = F_{tp} L U_{tp} \left(T_{c,tp} - T_{c,air}\right) \tag{2.2}$$

$$Q_{sub} = F_{sub} L U_{sub} \left(T_{c,sub} - T_{c,air}\right) \tag{2.3}$$

The term of F is the fraction of the relevant region and L is the length of the condenser channel. The term 'c' is used here to refer to caloric temperatures of air or refrigerant at each region. According to equations (2.1), (2.2) and (2.3), total heat transfer coefficient can be calculated as:

$$Q_{total} = Q_{dsh} + Q_{tp} + Q_{sub} \tag{2.4}$$

Another important topic of determination the pressure drops for refrigerant in the condenser. The same region assumption is considered, and pressure drop each of the indicated regions is obtained from equations below:

$$\Delta P_{dsh} = \frac{m_r^2}{A^2 \rho_g} - \frac{m_r^2}{A^2 \rho_{in}} + \left(b + \frac{C_{dsh}}{m_r^{.237}}\right) L \frac{F_{dsh}}{d} \frac{m_r^2}{2\rho_{in} A^2} \tag{2.5}$$

$$\Delta P_{tp} = \frac{m_r^2}{A^2 \rho_f} - \frac{m_r^2}{A^2 \rho_g} + \left(b + \frac{C_{tp}}{m_r^{.237}}\right) L \frac{F_{tp}}{d} \frac{m_r^2}{2\rho_f A^2} \tag{2.6}$$

$$\Delta P_{sub} = \frac{m_r^2}{A^2 \rho_{out}} - \frac{m_r^2}{A^2 \rho_f} + \left(b + \frac{C_{sub}}{m_r^{.237}}\right) L \frac{F_{sup}}{d} \frac{m_r^2}{2\rho_f A^2} \tag{2.7}$$

Finally, total pressure drops can be given as:

$$P_{total} = P_{dsh} + P_{tp} + P_{sub} \tag{2.8}$$

2.5.2.2. Evaporator Model

Two flow regimes of annular and dispersed are distinguished by the quality of refrigerant in the evaporator cold plate [3]. Annular regime is represented until the refrigerant quality reach up to 0.85, then dispersed flow regime is considered between 0.85 and 1.0. If refrigerant quality exceeds 1.0, this regime is called as superheated flow.

For annular flow regime, dispersed flow regime and single-phase superheated flow regime are calculated respectively by the help of equations below:

$$Q = m_r C_p (t_i - T_i)\left(1 - \exp\left(-\frac{UA_0}{m_r C_p}\right)\right) \tag{2.9}$$

$$Q = m_r C_p (1 - ANNUL)(t_i - T_i)\left(1 - \exp\left(-\frac{UA_0}{m_r C_p}\right)\right) \tag{2.10}$$

$$Q = \left(1 - \exp\left(-\frac{(1-ANNUL-XDRY)m_r C_p}{m_r C_p}\right)\right)\left(1 - \exp\left(-\frac{UA_0}{m_r C_p}\right)\right) \tag{2.11}$$

ANNUL is the fraction of heat exchanger in annular flow, on the same direction XDRY is used for the fraction in dispersed regime. They are defined as:

$$ANNUL = \frac{m_r (h_{0.85} - h_i)}{m_a C_p (t_i - T_i)}\left(1 - \exp\left(-\frac{UA_0}{m_r C_p}\right)\right) \tag{2.12}$$

$$XDRY = \frac{m_r (h_{out} - h_{inlet})}{m_a C_p (1-ANNUL)(t_i - T_i)}\left(1 - \exp\left(-\frac{UA_0}{m_r C_p}\right)\right) \tag{2.13}$$

2.5.2.3. Compressor Model

Heat transfer rate in evaporator is called the refrigeration capacity and it is denoted by Q_{in} [2]. These capacity values are obtained from the compressor property table. h_1 and h_4 are the enthalpy values of the evaporator inlet and compressor inlet respectively. $\dot{m}$ which is the mass flow rate of refrigerant could be identified as [1]:

$$\dot{m} = \frac{Q_{in}}{h_1 - h_4} \tag{2.14}$$

After the refrigerant flows inside the compressor, no heat transfer occurs in the compressor. However, the compressor gives an input power to sustain the process [1]:

$$\dot{W}_c = \frac{\dot{m}}{h_2 - h_1} \tag{2.15}$$

Another significant power is called an isentropic compressor power which assumes no entropy changes during the compressor process. In this equation, the term "h_{2s}" is the isentropic enthalpy value of the compressor outlet. The isentropic efficient of cycle also could be described with using this term:

$$\dot{W}_{2s} = \dot{m}(h_{2s} - h_1) \tag{2.16}$$

$$\eta = \frac{(h_{2s} - h_1)}{(h_2 - h_1)} \tag{2.17}$$

The coefficient of performance or COP is the ratio that is used to determine the useful cooling or heating energy needed to the compressor power. Generally, the cooling system is designed with a high COP value in order to create a highly efficient system and save the energy.

$$\mathrm{COP} = \frac{\dot{Q}_{in}}{\dot{W}_c} = \frac{(h_1 - h_4)}{(h_2 - h_1)} \tag{2.18}$$

The main four components are selected and numbered simultaneously, and different codes are written by EES for the results that are demonstrated in Table 2.7.

Table 2.7: EES Code Algorithm.

Evaporator Output Quality	x[1]=1
Evaporator Temperature	For 1. Case: T[1]= 20^{o}C +T_suph For 2. Case: T[1]= 10^{o}C +T_suph
Evaporator Pressure	P[1]=pressure(R$;T=T[1];x=x[1])
Evaporator Output Enthalpy (+Superheat)	h[1]=enthalpy(R$;T=T[1];P=P[1])
Evaporator Output Entropy	s[1]=entropy(R$;T=T[1];P=P[1])
Compressor Outlet Pressure	P[2]=pressure(R$;T=T_evap;x=x[1])
Compressor Outlet Temperature	T[2]=temperature(R$;P=P[2];h=h[2])
Compressor Outlet Enthalpy	h[2]=(wc/mdot)+h[1]
Compressor Outlet Entropy	s[2]=entropy(R$;h=h[2];P=P[2])
Isentropic Compression Entropy	s2s=s[1]
Isentropic Compression Enthalpy	h2s=enthalpy(R$;T=T[2];s=s[1])
Condenser Inlet and Outlet Pressure	P[3]=P[2]
Condenser Inlet Quality	x[3]=0
Condenser Temperature	T_cond=71^{o}C
Condenser Outlet Temperature	T[3]= 71^{o}C -T_sub
Condenser Outlet Entropy	h[3]=enthalpy(R$;P=P[3];T=T[3])
Condenser Outlet Enthalpy	s[3]=entropy(R$;P=P[3];T=T[3])
Condenser Load	Q_Con= mdot*(h[2]-h[3])
Evaporator Inlet Quality	x[4]=quality(R$;P=P[4];h=h[4])
Isenthalpic Expansion at Expansion Valve	h[4]=h[3]
Evaporator Inlet and Outlet Pressure	P[4]=P[1]

Table 2.8 shows the whole equations to be transferred to EES.

Table 2.8: Ideal Vapor Compression Cycle Equations.

Compressor Power	W_c= Getting from Table 2.6
Cooling Capacity	Q_{in}= Getting from Table 2.5
COP	$= \frac{\dot{Q}_{in}}{\dot{w}c} = \frac{(h_1 - h_4)}{(h_2 - h_1)}$
Mass Flow Rate	$\dot{m} = \frac{\dot{Q_{in}}}{(h_1 - h_4)}$
Isentropic Compressor Power	$\dot{m}(h_{2s} - h_1)$

After the calculation of codes, the mass flow rate and quality of the evaporator values, which can be obtained from this chapter are conveyed to Matlab to create a code.

3. MATHEMATICAL MODEL of EVAPORATOR

3.1. Sizing of the Evaporator

The evaporator allows the two-phase refrigerant which consists of liquid and vapor to convert to a single-phase refrigerant by taking heat from the inside of a place depending on refrigeration system quality, thus it provides the key cooling process for the place. This working principle illuminates the sizing of the evaporator. The operating and initial conditions should be needed to calculate the evaporator properties before the determination of equations and relations between system components. The whole data of refrigeration system could be thermodynamically obtained by using software called EES. Table 3.1 and Table 3.2 show the varying initial conditions for the sizing of evaporator.

Table 3.1: Initial Conditions for The First Case (Evaporator Temperature: 10^{o}C).

The pressure of refrigerant at the evaporator inlet [kPa]	P_{evap}= 414.9
The temperature of refrigerant at the evaporator inlet [K]	T_{evap_in}= 283
The superheat temperature of refrigerant [K]	T_{evap_out}= 288
The quality of refrigerant at the evaporator inlet	x_{in}= 0.44
The mass flow rate of refrigerant of one evaporator $\left[\frac{kg}{s}\right]$	$\dot{m}$= 0.002245

Table 3.2: Initial Conditions for The Second Case (Evaporator Temperature: 20^{o}C).

The pressure of refrigerant at the evaporator inlet [kPa]	P_{evap}= 572.1
The temperature of refrigerant at the evaporator inlet [K]	T_{evap_in}= 293
The superheat temperature of refrigerant [K]	T_{evap_out}= 298
The quality of refrigerant at the evaporator inlet	x_{in}= 0.39
The mass flow rate of refrigerant of one evaporator $\left[\frac{kg}{s}\right]$	$\dot{m}$= 0.002135

These differences between both tables are caused by the changes of the evaporator temperature. Due to this data, the density, viscosity, specific volume of refrigerant could be calculated for the single and two-phase flows by Coolprop

Toolbox which is an addition to Matlab. The operating conditions also are shown in Table 3.3.

Table 3.3: Operating Conditions of Components.

The Cooling Load of One Evaporator	180 W
The optimum temperature of wall as a result of the computer work	348 K
The optimum ambient temperature	336 K

3.2. Evaporator Calculation

In this study, the evaporator channel is designed as a circular, because non-circular channel needs to require more energy to pump refrigerant through it than the circular channel due to friction. Additionally, circular section decreases the effect of internal stress on the channel walls and it can be produced with using less material in its construction per unit lengths.

"D" and "L" symbolize respectively the outside diameter and the length of the evaporator channel. They are used to find the pressure drop of evaporator and the temperature distribution of the evaporator channel and walls due to heat transfer coefficient.

D value is selected as 5 mm considering the mini channel application. The inlet diameter can be obtained by subtracting the wall thickness from the outside diameter of channel.

$$\mathrm{D_{internal}} = (\mathrm{D} - \text{Wall Thickness}) x 10^{-3}\ [m] \tag{3.1}$$

L value is estimated with a valid interval in order to get preliminary design parameters for the evaporator channel. Average heat transfer coefficient and average temperature difference between the refrigerant and the channel wall are given to the equation to find the relation of result and L value. If both values have matched each other, L value can be used during the process.

$$Q_{Coo.Cap} = h_{ort} \frac{\pi DL}{2} (\Delta T_{ort}) \quad [kW] \tag{3.2}$$

The cross area of the channel could be defined as:

$$A_{Kesit} = \frac{\pi * D_{int}{}^{2}}{4} \; [m^2] \tag{3.3}$$

The mass flow rate of the refrigerant is obtained by:

$$G = \frac{\dot{m}}{A_{Kesit}} \quad \left[\frac{kg}{m^2 s}\right] \tag{3.4}$$

Before the examination to appropriately design the evaporator with the relation of temperature and pressure, the characteristic of the refrigerant in the evaporator need to be explained. The refrigerant which is removed the pressure by the expansion valve, enters to the evaporator as liquid-vapor mixture and later, the heat is absorbed by the refrigerant in the evaporator. The liquid phase of the refrigerant turns into the vapor phase due to this reaction. The refrigerant in the evaporator should be divided into two main regions: The single-phase region and two-phase region.

Both regions mostly have the different properties. The two-phase region occurs naturally where the quality has a value between 0 and 1. These values can be called as the saturated liquid and saturated vapor respectively. In this study, the two-phase region is considered as the inlet of the evaporator and the liquid vapor mixture continues to flow through the evaporator until the quality value reaches the 1. Therefore, the liquid and vapor phases of the refrigerant should be examined separately.

Essentially, the Reynolds Number of liquids should be needed to find the flow regime. If the Reynolds Number is less than 2300, the flow is called as laminar. If not so, it is the turbulent flow [5].

$$Re_{liq} = \frac{G * D_{int} * (1 - x)}{\mu_l} \tag{3.5}$$

- $\mu_l = Dynamic\ Viscosity\ (For\ liquid)\ [\frac{kg}{ms}]$

The same process should be applied to the vapor in order to determine the laminar or turbulent assumption [5].

$$\mathrm{Re_{vap}} = \frac{\mathrm{G*D_{int}*x}}{\mu_v} \tag{3.6}$$

- μ_v: $Dynamic\ Viscosity\ (For\ vapor)\ [\frac{kg}{ms}]$

The Fanning Friction Factor is calculated in two-phase region for both flow regimes. This factor is defined as the ratio between the local shear stress and the local flow kinetic energy density. For laminar regime [18]:

$$\mathrm{f_l} = \frac{16}{\mathrm{Re}} \tag{3.7}$$

For turbulent regime [18]:

$$\mathrm{f_{turbulance(liquid\ or\ vapor)}} = \frac{1}{[3.64\ln(Re_v)-3.28]^2} \tag{3.8}$$

The pressure drop of liquid can be obtained with using the FFF [18] :

$$\Delta \mathrm{P_{tp_{liquid}}} = L_{tp} * \frac{2*f_l*G^2*(1-x)^2}{D_{int}*\rho_l} \tag{3.9}$$

- L_{2p} : $The\ length\ of\ the\ two\ phase\ region$
- ρ_l : $The\ density\ of\ liquid\ R-134a$

The pressure drop of vapor is calculated as [18] :

$$\Delta \mathrm{P_{tp_{vapor}}} = \mathrm{L_{tp}} * \frac{2*\mathrm{f_v}*\mathrm{G}^2*(\mathrm{x})^2}{\mathrm{D_{int}}*\rho_v} \tag{3.10}$$

- L_{2p} : $The\ length\ of\ the\ two\ phase\ region$
- ρ_v : $The\ density\ of\ gas\ R-134a$

Additionally, the acceleration pressure drop occurs due to velocity difference between gas and liquid [5] :

$$\Delta \mathrm{P_{acc}} = (\mathrm{x_{n+1}} - \mathrm{x_n}) * \mathrm{v_{lv}} * \mathrm{G}^2 \tag{3.11}$$

- v_{lv} : $Specific\ volume\ \left(\frac{m^3}{kg}\right)$
- n : $Number\ of\ process\ steps$

After the determination of the pressure drops, some dimensionless quantity should be identified to calculate the heat transfer coefficient. These terms, which are the Convection Number, Boiling Number and Froude Number provide a basis of the Shah's correlation [18].

The Convection Number can be defined as:

$$\mathrm{Co} = \left(\frac{\rho_g}{\rho_l}\right)^{0.5} \left(\frac{1-x}{x}\right)^{0.8} \tag{3.12}$$

The Boiling Number is defined as:

$$\mathrm{Bo} = \frac{q''}{G * h_{lg}} \tag{3.13}$$

The Froude Number is described as:

$$\mathrm{Fr_{lo}} = \frac{G^2}{\rho_l^2 * g * D_{int}} \tag{3.14}$$

These parameters can be used in the different ranges of Reynolds Number for liquid [18] :

$$h_{lo} = \frac{Re_{lo} * Pr_l * \left(\frac{f}{2}\right) * \left(\frac{k_l}{D_{int}}\right)}{1.07 + 12.7\left(Pr^{\frac{2}{3}} - 1\right) * \left(\frac{f}{2}\right)} \qquad 2300 \leq Re_{lo} \leq 5x10^6 \tag{3.15}$$

The friction factor in this equation is given as [18]:

$$f = \frac{1}{[1.58 \ln(Re_{lo}) - 3.28]^2} \tag{3.16}$$

The Prandtl Number is a dimensionless number which defines as a ratio of the momentum diffusivity to the thermal diffusivity. The Prandtl Number for liquid:

$$\mathrm{Pr_l} = \frac{\mu_l C_p}{k_l} \tag{3.17}$$

The two-phase heat transfer coefficient is obtained from using the equations below. The Kandlikar correlations consists of the convective and nucleate boiling terms which belong to boiling process of refrigerant. The correlation for two phase heat transfer coefficient is given as [18]:

$$\frac{h_{tp}}{h_{lo}} = [0.6683\mathrm{Co}^{-0.2}.\mathrm{f_2(Fr_{lo})} + 1058\mathrm{Bo}^{0.7}.\mathrm{F_{fl}}] * (1-\mathrm{x})^{0.8} \tag{3.18}$$

$$\frac{h_{tp}}{h_{lo}} = \left[1.136Co^{-0.9}.f_2(Fr_{lo}) + 667.2Bo^{0.7}.F_{fl}\right] * (1-x)^{0.8} \tag{3.19}$$

The larger value is considered for the future equations. The definition of $f_2(Fr_{lo})$ term in this equation can be [18] :

$$f_2(Fr_{lo}) = (25Fr_{lo})^{0.3} \qquad \mathrm{Fr_{lo}} < 0.4 \tag{3.20}$$

$$f_2(Fr_{lo}) = 1 \qquad \mathrm{Fr_{lo}} > 0.4 \tag{3.21}$$

$\mathrm{F_{fl}}$ is the surface parameter that depends on the refrigerant and the heat transfer surface. Table 3.4 below shows the values for several different refrigerants.

Table 3.4: Surface Parameter of Different Refrigerant.

Refrigerant (Fluid)	$\mathrm{F_{fl}}$
Water	1.00
R-11	1.30
R-12	1.50
R-134a	1.63
R-132	3.30

The next step is to determine the effects of single-phase region on the pressure drop. The approaches in the two-phase region should be applied to this region.

The Reynolds Number of single phase can be defined as [19] :

$$\mathrm{Re_v} = \frac{G*D_{int}}{\mu_v} \tag{3.22}$$

The FFF for single phase:

$$f_d = \frac{16}{Re_v} \tag{3.23}$$

The heat transfer coefficient for single phase laminar flow [16] :

$$h_{single} = \frac{k_v}{D_{int}} * \frac{3.657+(0.0677*Re*Pr*\left(\frac{D_{int}}{L}\right)^{1.33}}{1+0.1*Pr\left[Re*\left(\frac{D_{int}}{L_{single}}\right)\right]^{0.3}} \tag{3.24}$$

For turbulent flow [19] :

$$h_{single} = Nu\frac{k_v}{D_{int}} \tag{3.25}$$

For Reynolds number in range of 10^3<Re< $5x10^6$ and Prandtl Number in range of 0.5<Pr<1, Nusselt Number can be defined with using Gnilinski Correlation.

$$Nu = \frac{f}{2} * \frac{(Re-1000)*Pr}{1+12.7*\sqrt{\left(\frac{f}{2}\right)\left(Pr^{\frac{2}{3}}-1\right)}}\left(\frac{T_b}{T_w}\right)^{n=\frac{1}{3}(refrigerant)} \tag{3.26}$$

Pr is Prandtl Number and it can be calculated as:

$$Pr = \frac{\mu_v C_p}{k_v} \tag{3.27}$$

Last term of equation 3.26 is used as a safety factor to minimize the changeable properties.

The pressure drops of the single phase region can be found as [19]:

$$\Delta P_{single} = 4 * f_d * \frac{1}{D_{int}} * \frac{G}{2*\rho_l} \tag{3.28}$$

For the purpose of comparison, the temperature distribution on the side walls should be needed.

$$Q_{evaporator\ C.C} = UA * (T_s - T_m) \tag{3.29}$$

In this equation, T_s is a wall temperature and T_m defines the refrigerant temperature along the evaporator. In addition to these terms, T_1 is used to indicate the temperature value of the circular copper channel.

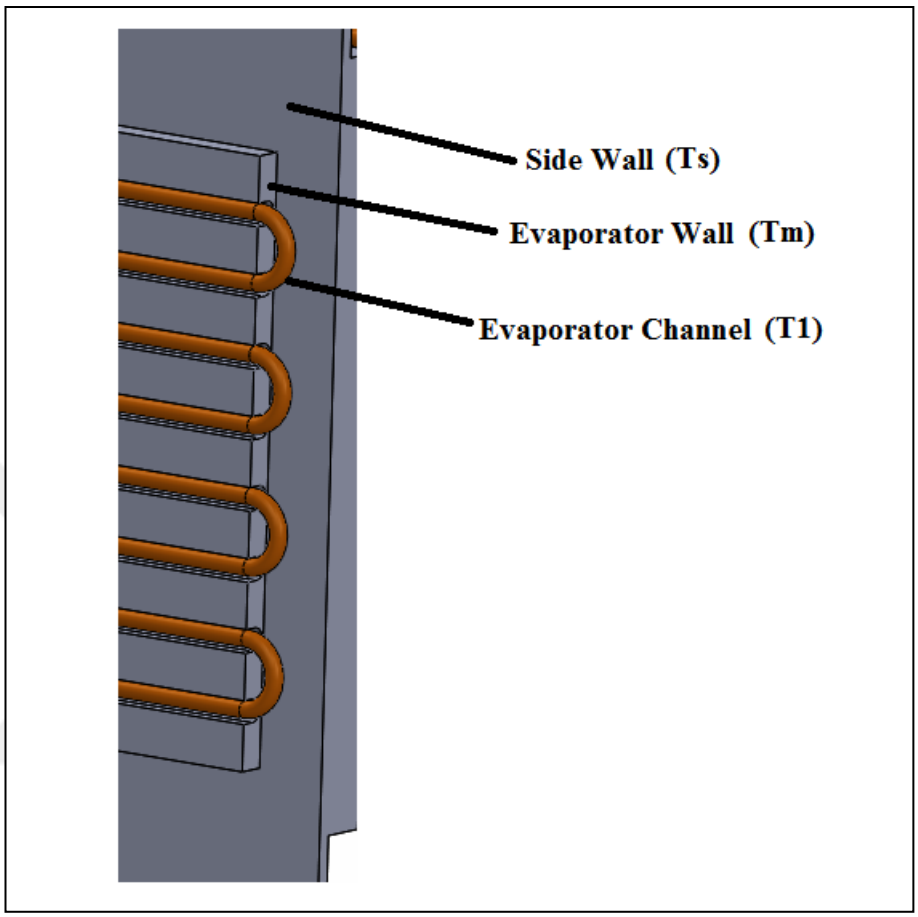

Figure 3.1: Parts of Equation 3.28.

UA term can be defined as a resistance:

$$UA = R_{cont.loss} + \frac{1}{h_{cor} * \left(\frac{\pi * D_{int} * L}{2}\right)} + \frac{\ln\left(\frac{D}{D_{int}}\right)}{\pi * k_{copper} * L} + \beta * \frac{\frac{t}{D/2}}{\pi * k_{Al} * L} \quad (3.30)$$

The first term from this equation occurs due to the contact between the circular pipe and wall. They cannot smoothly contact each other. Therefore, the average losses for this term should be defined as:

$$R_{cont.loss} = 0.05 * 10^{-4} \left[\frac{m^2 K}{W}\right] \quad (3.31)$$

The contact region between the refrigerant and wall is described in the second term. The half of the total area is considered as the contact region.

h_{corr} which is another parameter of the second term, is used to establish a relationship between the single phase and two-phase heat transfer coefficients. Thus, a safe working principle can be provided.

$$h_{corr} = h_{tp} + h_{single} \tag{3.32}$$

The third term demonstrates the heat conduction between the inner and outer diameters of the circular pipe. k is a thermal conductivity coefficient of the selected material. For copper, its value is 385 W/m.K.

The last term from this equation is used to define the heat conduction between the wall and pipe. t is called as a wall thickness, k is a thermal conductivity coefficient of the wall and it is 199 W/m.K for aluminum material. Beta is also used as a safety factor which is calculated by the approach.

3.3. Design of the Cold Plate

As implied above, the purpose of the study is obtained the optimum results with the minimum errors. The main part of this case is the cooling capacity.

In this direction, the several data could be used to get overall heat transfer coefficient which is one of the significant parameters. Insulation of external environment conditions and the heat transfer coefficients according to the phases of refrigerant play the important role as a parameter and assumption.

Another detail of this study, the circular channel cannot completely contact with all the side walls. The geometry difference between the channel and the contact region of the side wall causes the losses and faults. Hence, it should be considered that the air particles fill the gap in the contact surface.

All of these reasons, the specific safety factor should be determined to sustain the sizing process and obtain the desirable dimension values from the system.

Cold plates in this study are produced and placed considering the safety factor. Additionally, they are designed with the support blocks which are used to provide a zone for the cards. They have different dimensions and it is shown in Figure 3.2.

Figure 3.2: Support Blocks of Cold Plate.

4. SELECTION of OTHER COMPONENTS

4.1. Condenser Selection & Production

Condenser is a type of heat exchanger that makes a phase change of fluid. Similarly, all its types are used to condense the refrigerant from the vapor to saturated liquid state.

There is a strong connection between the condenser and the fan in the course of working process. The fan blows the air through the condenser fins and tubes. Thus, the refrigerant in the condenser can lose its heat depending on the forced convection heat transfer.

The selection of the condenser could be done by the helps of other components and thermodynamic properties of system. Eventually, it is determined that the air-cooled condenser working principle is suitable for this process. This type of condenser could provide:

- The high heat transfer rate
- 30 percent more than the internal and external heat transfer coefficients
- The low pressure drops
- Smaller internal volume
- Lighter than other types of condenser.
- In addition to these properties, this type of condenser has a wide operating temperature range of -60 ^{o}C to 125 ^{0}C.

In this study, Sanhua SD Microchannel Heat Exchanger is selected to maintain the cooling cycle process considering the conditions above. The operating conditions of this condenser can be seen from Table 4.1.

Table 4.1: Sanhua SD Microchannel Heat Exchanger Properties.

Operating Ambient Temperature Range	-30 ^{o}C to 72 ^{o}C
Operating Temperature Range of Refrigerant	-60 ^{o}C to 121 ^{o}C
Design Pressure	4.5 MPa
Tube Number	20

The picture of Sanhua SD Microchannel Heat Exchanger is shown in Figure 4.1.

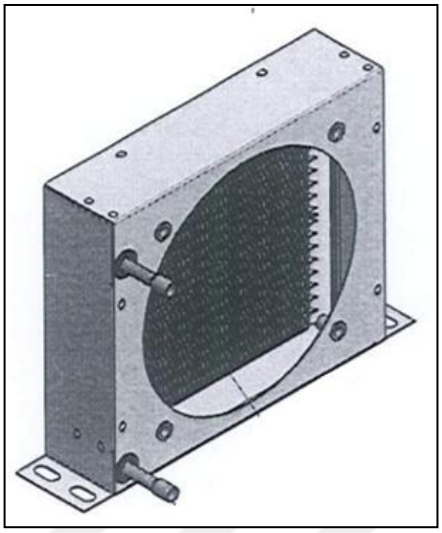

Figure 4.1: The view of Sanhua SD Microchannel Heat Exchanger.

4.2. Fan Selection

The fan is a significant part such as the main components of refrigeration system. Due to this reason, the selection of the fan should be done carefully. The fan should provide a reliable and sustainable source under operating conditions.

The most important criteria for the selection of the fan are:

- Fan Dimension
- Fan Weight
- Operating Temperature Range
- Condenser Capacity
- Airflow

The fan is placed into the computer and related to the condenser, therefore it should be properly chosen in order to give an opportunity to efficiently and simultaneously work on a wide range of condenser capacities. Fan that can would be used in this study is selected considering the limitations and selection criteria above to properly design a robust system.

It can be categorized into two main classes considering the air flow: Axial Flow Fan and Centrifugal Fan. Axial flow fan is preferred with suitable for equipment with small ventilation system.

First selected and preferred fan is called as DC axial compact fan 6314 /2 TDHHP. It can be worked efficiently for a smooth operation. Moreover, it weights approximately 1000 g and dimensionally provides the working area to do research with the miniature system.

Its critical properties can be seen from the Table 4.2.

Table 4.2: Main Features of DC axial compact fan 6314/2 TDHHP.

Fan Type	Dimension and Depth (mm)	Nominal Voltage (V)	Air Mass Flow Rate (m^3/h)	Operating Temperature Range (^oC)	Mass (g)
DC axial compact fan 6314/2 TDHHP	172*51	24	710	-20.....75	910

The relation between pressure and air mass flow rate is used for making an explanation about the optimum working area of the fan. As seen below, the shaded area under the curve explains the optimum operating area of the fan. Thus, it plays an important role in responding to fan needs. The blue hatched area in Figure 4.2 presents the same result for 6314/2 TDHHP fan.

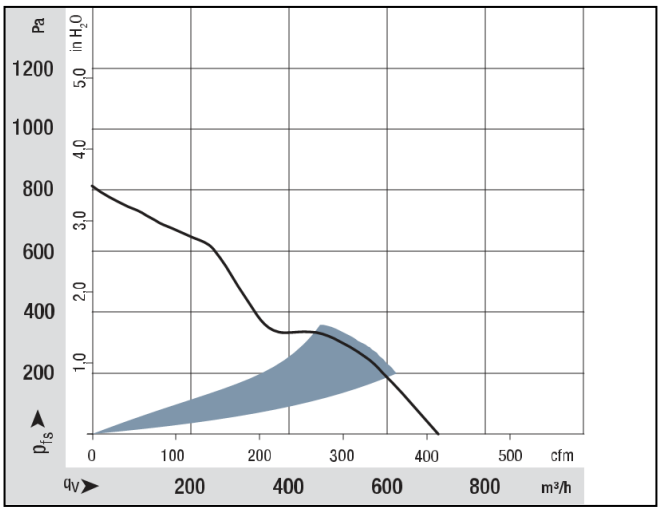

Figure 4.2: Optimum Working Area of 6314 /2 TDHHP fan.

DC axial fan 6314N/2 TDHHP, the other alternative fan, is less than about 1000 g. It can be chosen to work with high efficiency on the miniature system. Additionally, it has a same dimension and shape with others. Table 4.3 provides the whole properties of fan.

Table 4.3: Main Features of DC Axial Fan 6314N/2 TDHHP.

Fan Type	Dimension and Depth (mm)	Nominal Voltage (V)	Air Mass Flow Rate (m^3/h)	Operating Temperature Range (^oC)	Mass (g)
DC axial compact fan 6314N/2 TDHHP	172*51	24	970	-20.....70	850

It can be seen from the data in Figure 4.3 that DC axial fan 6314N /2 TDHHP provides the wide range of optimum working area than first one.

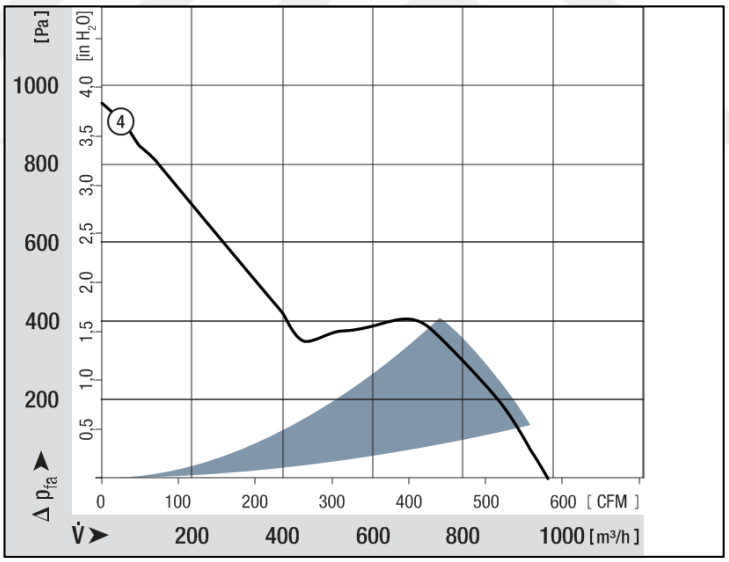

Figure 4.3: Optimum Working Area of DC Axial Fan 6314N /2 TDHHP.

Another type of DC axial fan 6314 /2 TDHHP-298 is selected to be an alternative to others. The weight and dimension of this fan is similar to the others. Main features are shown in Table 4.4.

Table 4.4: Main Features of DC Axial Fan 6314 /2 TDHP-298.

Fan Type (DC Axial)	Diameter(mm)* Depth (mm)	Nominal Voltage	Air Flow Rate (m^3/h)	Temperature Range (^0C)	Weight (gr)
DC axial fan 6314 /2 TDHP-298	172*51	24	600	-20.....65	910

The relation between the fan flow rate and pressure is investigated same as before in Figure 4.4.

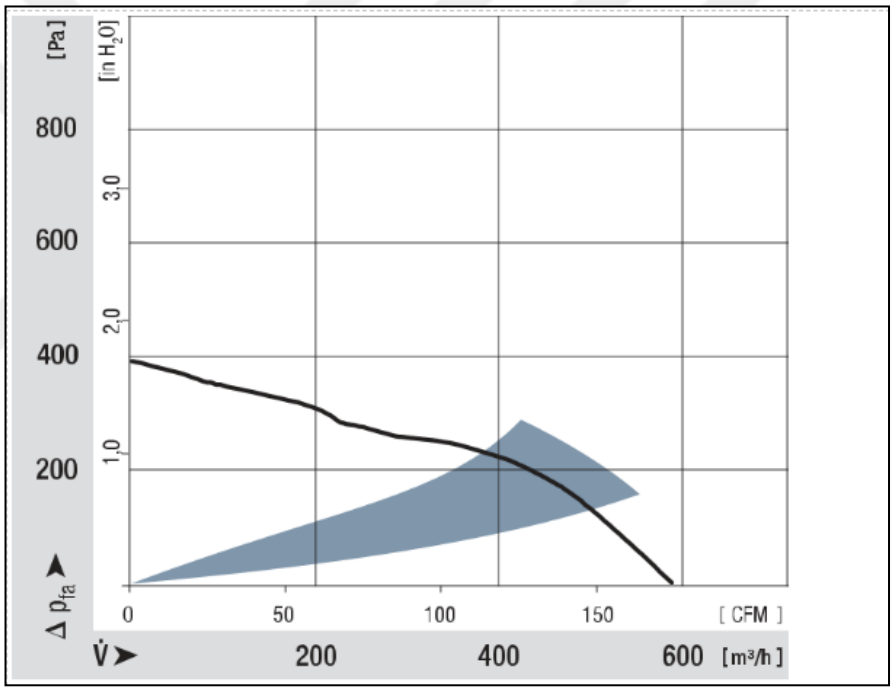

Figure 4.4: Optimum Working Area of DC Axial Fan 6314 /2 TDHP-298.

After making a comparison among these types of fan, 6314/2 TDHHP become more suitable than others due to its optimum working area and other properties.

4.3. Selection of Expansion Valve and Other Components

Before moving to next step, the expansion valve, the last main component, should be selected and placed in order to regulate the cycle.

Expansion valve can reduce the pressure of cooling cycle from condenser pressure level to evaporator pressure level. There are numerous types of expansion valve depending on its control system: Thermal expansion valve, Electronic Expansion Valve and Automatic Expansion Valve [20] .

Thermal expansion valves are popular and used commonly at a high temperature range and desirable high capacity. However, when it is used in the high superheat process, it steals the heat transfer area from evaporator during the evaporation process.

Electronic expansion valves, which are another type of expansion element, are consisted of the sensors, regulator, actuator and the valve itself. They can handle large variations in operating conditions and they are also controlled by pressure or temperature sensor. For this reason, the covered working area is not applicable for the miniature application and they are mostly found on very large systems. Its cost is higher than other devices as well.

Automatic expansion valves have several essential properties that can be used efficiently with this project. These properties can be listed as:

- Small dimensions
- High performance
- Hermetic construction
- Adjustable evaporating pressure setting etc.

In this study, Honeywell Series AEL- Automatic Expansion Valve is used to maintain and sustain the cooling cycle. Addition to the properties above, it can be worked with the maximum pressure of 25.5 bar and maximum test pressure of 28 bar. It can also be worked within 100^{o}C of the ambient temperature. The expansion valve is illustrated in Figure 4.3.

Figure 4.5: Honeywell Expansion Valve.

Dryer is an assistant element which is placed between the condenser outlet and expansion valve inlet.

Sightglass has a wide temperature range of -40°C to over +120°C and it is used to make an observation of the refrigerant in the piping system.

4.4. Pressure and Temperature Sensors

AKS 32R pressure sensor gives an opportunity for working with a miniature system in the course of a cooling process. This sensor converts the measured pressure to the linear output signal. Thus, it can make a connection between itself and system.

The main features of AKS 32R can be seen from Table 4.5.

Table 4.5: Properties of Selected Pressure Sensor.

Product	AKS 32R
Operating Temperature Range	−40 to 85°C
Ambient Temperature	90°C
Operating Pressure Range	1 to 12 bars
Compensated Temperature Range	-30 to +40
Weight	0.15 kg

Temperature plays a vital role in many industrial processes like cooling and therefore an accurate measurement is a must. The temperature of the system can be measured using the temperature sensor.

In this study, PT 100 the most common type of thermometer is placed several points of cycle depending on measuring principle of sensors. The main features which cause to select this sensor are shown in Table 4.6.

Table 4.6: Properties of Selected Temperature Sensor.

Product	PT 100
Operating Temperature Range	-50°C to 230°C
Standard length	500mm ± 1%
Nominal resistance	100 Ω at 0°C (Pt 100)

5. TEST BENCH DESIGN

5.1. Cartridge Heater Production

After the computer is designed satisfying a set of requirements, the experimental analysis with this computer can be conducted in order to collect the correct and reliable data. Hence after the extensive research, cartridge heater is found appropriate to obtain the equal power from them like the cards.

Cartridge heaters are located on the plate that is used for forming contact region between cold plate blocks. From, respectively, Table 5.1 and Table 5.2, the needed power and measured dimensions are set out for each plate.

Table 5.1: Power Requirement of Each Plate.

Source	Power (W)
Plate 1	45
Plate 2	45
Plate 3	45
Plate 4	75
Plate 5	10
Plate 6	15
Plate 7	10
Plate 8	5
Plate 9	110

Table 5.2: Dimensions of Each Plate.

Plate 1-8	Thickness: 4.7 mm
	Width: 234 mm
	Height: 160 mm
Plate 9	Thickness: 25.5 mm
	Width: 234 mm
	Height: 160 mm

Every cartridge heater block has 40 W of heat power; hence two or three cartridge blocks can be used for one plate to reach the desirable values. When they are placed to the computer cabin, they are in a position such as Figure 5.1.

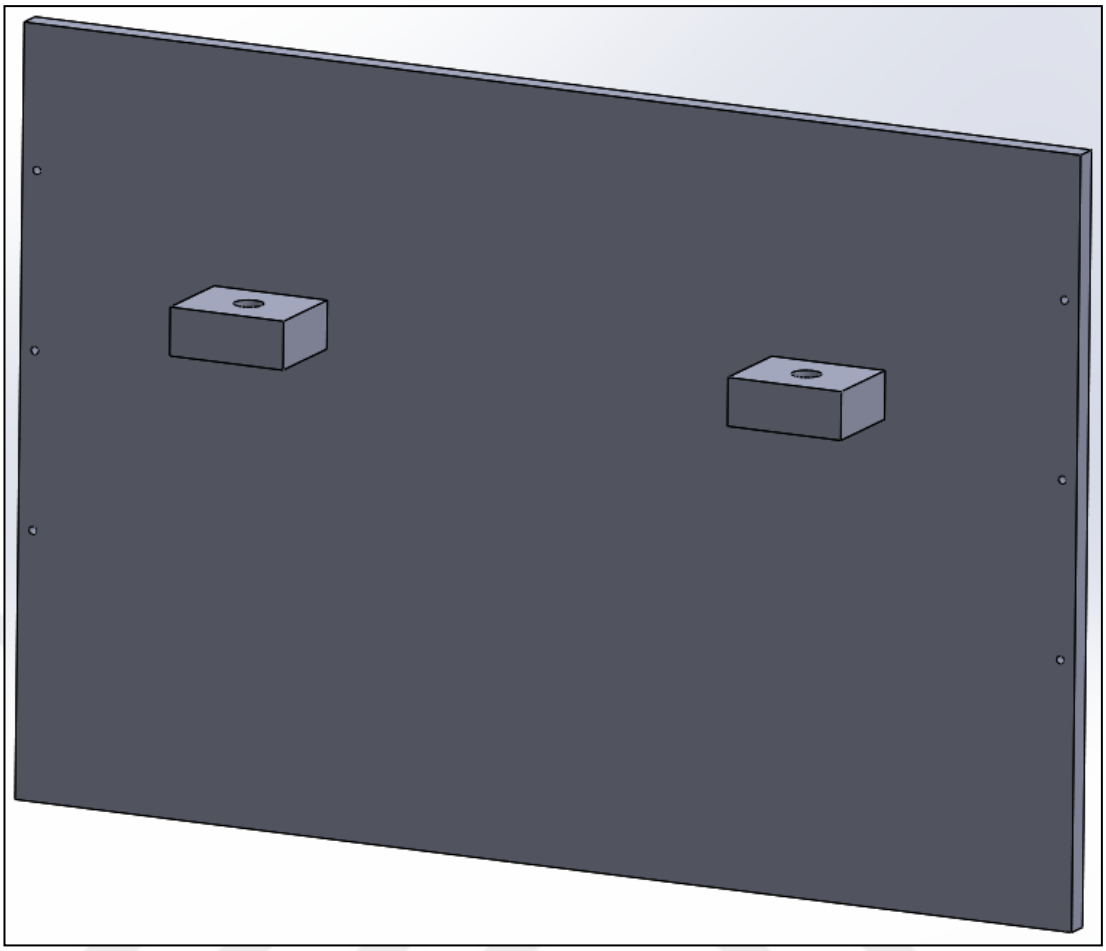

Figure 5.1: Plate Resistances and Their Connections in the Computer Cabin.

5.2. Piping and Instrumentation Diagram of Cooling Cycle

After selection of the components, they should be placed and maintained in the proper location in order to obtain sustainable advantages from the cooling system.

The piping and instrumentation diagram demonstrate the information about the equipment of the system such as pipes, fittings and main components. It is denoted by P&ID and used to create important documentation for a process flowchart. Each equipment has a unique symbol in the P&ID, thus the cooling cycle can be described with the help of them.

As the first step, two evaporators are positioned along the side walls of the computer cabin. The front of the computer cabinet consists of two parts: First part maintains the compressor, dryer, sightglass and expansion valve together. In the same direction, second part has the micro-channel condenser and selected fan which locates in the wall.

For the second step, cold plates and cartridge heaters are assembled into the computer cabin.

Last step, the pressure and temperature sensors which are used to measure the critical thermodynamic properties of system, can generally be located on the outlet of evaporator, the outlet of the compressor and the outlet of condenser. Addition to them, eight of temperature sensors are positioned in the computer cabin.

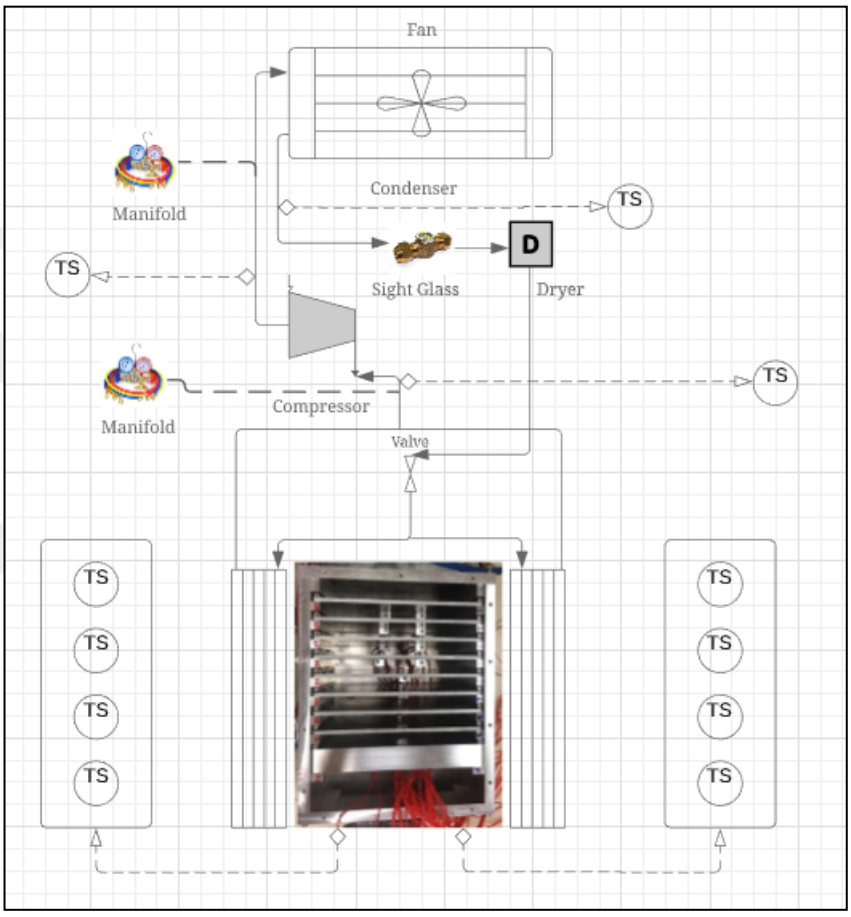

Figure 5.2: The Piping and Instrumentation Diagram of Computer Cooling System.

5.3. Electronic Components and Wiring Diagram

The electronic connection of the system can be listed as follows: Electrical Panel, Inside of the Computer, Outside of the Computer and Host Computer Link.

Electrical panel region has the main electronic components of the system such as processor, drivers, power supplies, digital potentiometer and compressor driver board. The processor of the system is called as ARM Cortex-M MCU and it is

connected to the digital potentiometer with 5 V. Other essential connection is between itself and four Mosfet which is controlled by PWM. According to One Wire Pin Protocol, the processor can gain access to temperature sensors which 18 of them are located inside, 6 of them are found outside of the computer cabin.

Mosfet ,which provides an opportunity to work at desired values with cartridge heaters, is connected to the 12 V Switch Mode Power Supply (SMPS). It is used for switching at high frequency. This system does not require the high frequency; therefore, it can be controlled by Optocoupler.

Digital potentiometer has a connection with processor and compressor driver board. Thus, it can allow people to control the compressor speed. Compressor driver board is also connected both to compressor and 24 V SMPS.

SMPS is the power supply of this study. It can be worked at high elevated temperature and high power. 12 V SMPS is only connected to Mosfet boards, however 24 V SMPS is both linked to compressor driver board and fan.

Thermal sensors, located in computer cabin to measure temperature values, are connected to the processor and in contact with side walls. Cartridge heater, which are linked to Mosfet board, transmit the power from SMPS to heater blocks and aluminum plates in order to generate the homogeneous thermal distribution.

The region, which is called as the outside of computer cabin, has the cooling cycle components and thermal sensors, which are found on the pipe.

FTDI programme board is used for creating link between electrical panel and host computer.

Figure 5.3 shows the wiring diagram of system.

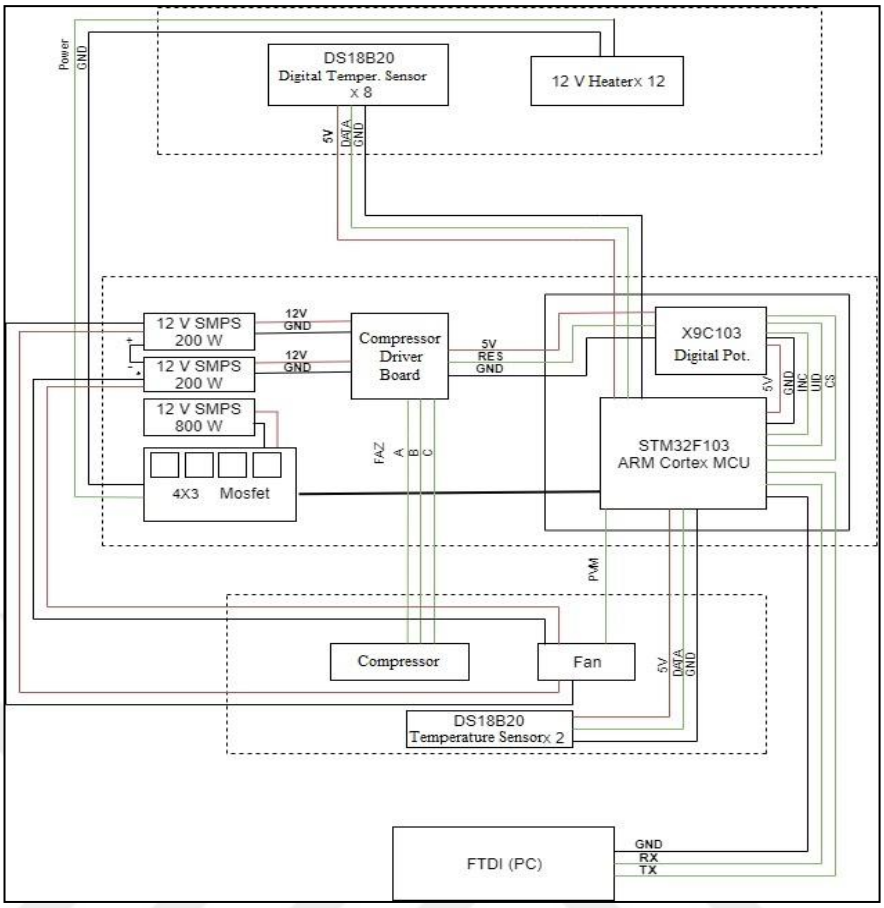

Figure 5.3: Wiring Diagram of Cooling System.

5.4. Design of the Test Bench and Management System

After the sizing and selection of the components, they are brought together to simulate the refrigeration system and check the results getting from mathematical model. The reference of the test bench in this study could be seen in Figure 5.4 [21].

Figure 5.4: Example of The Test Bench Equipped with The Evaporator.

First of all, this computer cabinet is designed including the cold plates in which the cards are placed. This drawing is shown in Figure 5.5.

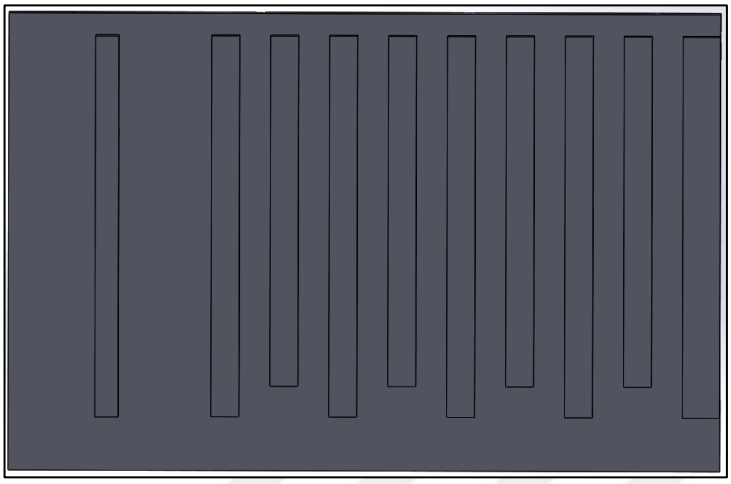

Figure 5.5: Sketch of the Cold Plates and Side Wall.

On the test bench, the plate resistances are used to supply the heat generation for the computer, instead of using the power cards. This equipment minimizes the heat losses due to convection, because the heat transfer between the plate resistances and the walls occurs predominantly by conduction.

The evaporator is designed considering its dimension values which are obtained from Matlab results. Thus, the experimental analysis on the test bench could be compared with the mathematical model of refrigerant system. The evaporators are placed next to the side walls. Figure 5.6 presents this placement.

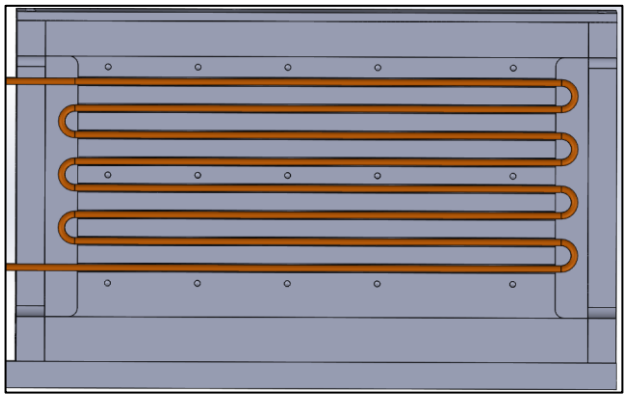

Figure 5.6: Side Walls and Evaporator.

All other components of refrigeration system except the evaporator are placed

the backside of the computer. The dimension of the backside of the computer is adjusted to fit the components into the computer. Additionally, one thin plate is placed in contact between the compressor and the condenser Thus, it divides the computer into two different parts in order to be efficiently worked.

Again, the ventilation hole is opened at the backside of the computer to continuously provide the air circulation. Thus, the fan can be worked simultaneously with the condenser. Other cooling components such as dryer, sight glass etc. are connected with the main part. (Figure 5.7)

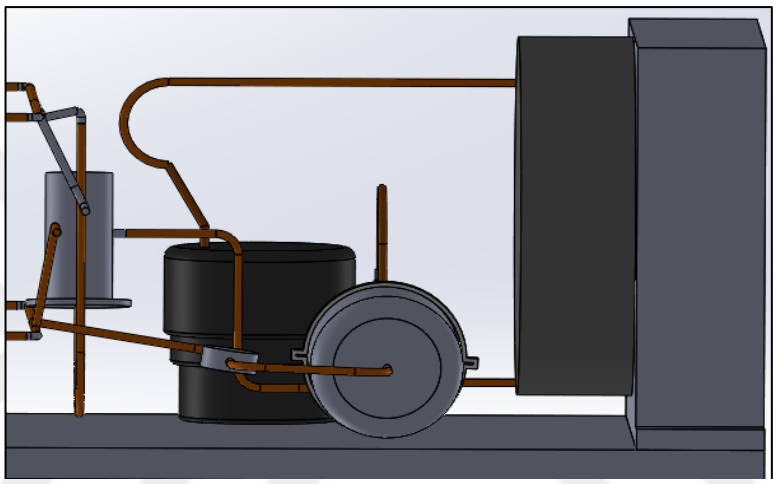

Figure 5.7: Placement of Cooling Equipment.

All parts of computer and other refrigeration system components are assembled in Figure 5.8 according to the P&ID.

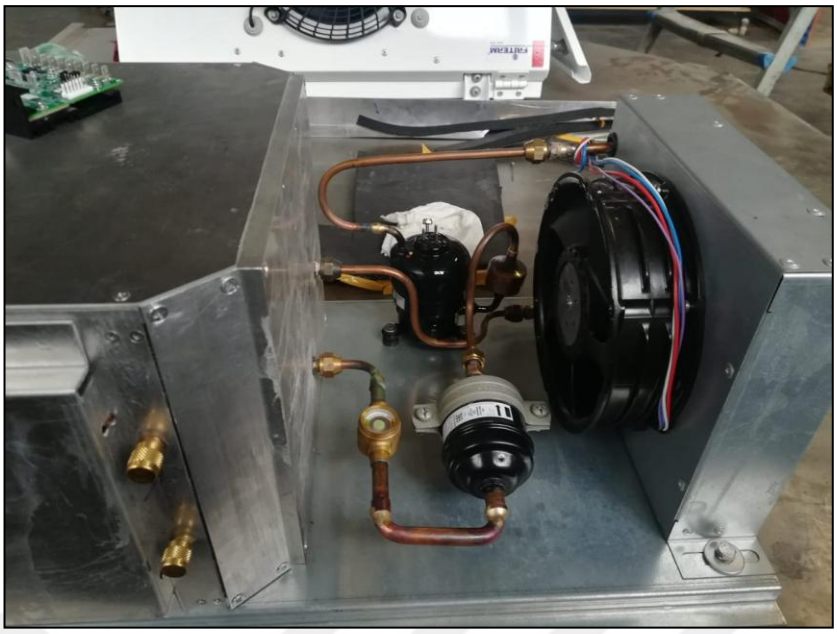

Figure 5.8: The View from Test Bench

After test bench design, management system should be designed to obtain information creating thermodynamic properties relation diagrams, especially for changing values of temperature and pressure.

5.5. List of Conducted Tests

The ambient temperature plays a critical role for conducting analysis. All tests are conducted at room temperature (25 ^{o}C), at optimum operating temperature of compressor (40 ^{o}C) and at desired operating temperature (55^{o}C).

Under different temperature conditions, the system should be worked at half thermal load and at full thermal load depending on operating time (steady analysis). On the other hand, same tests with same loads are repeated at transient analysis. Thus, these tests will not be time dependent.

Addition to these findings, voltage and current values of fan, compressor power, the operating points of compressor and fan should be obtained from test results.

Tests to be conducted can be listed as in Table 5.3.

Table 5.3: Data Sheet for Tests.

Time Dependence	Steady			Transient		
Ambient Temperature	25 ºC	40ºC	55ºC	25ºC	40ºC	55ºC
Load Case 1 (Thermal Load)	at Half Power	at Half Power	at Half Power	at Half Power	at Half Power	at Half Power
Load Case 2 (Thermal Load)	at Full Power	at Full Power	at Full Power	at Full Power	at Full Power	at Full Power
Load Case 3 (Thermal Load)	Both at Full Power (30 min) and at Half Power (30 min)	Both at Full Power (30 min) and at Half Power (30 min)	Both at Full Power (30 min) and at Half Power (30 min)	Both at Full Power (30 min) and at Half Power (30 min)	Both at Full Power (30 min) and at Half Power (30 min)	Both at Full Power (30 min) and at Half Power (30 min)

6. RESULTS

6.1. Thermodynamic Properties

Based on the EES code which is mentioned in previous chapters, thermodynamic properties of the cooling cycle are calculated by considering the operating condition. They also should meet the compressor conditions to retain control over cycle. As a result of the calculation of the thermodynamic properties, the cycle points are determined at 2463 RPM and evaporator temperature of 20^{o}C.

The results of the enthalpy, pressure, entropy and temperature values are presented in Table 6.1.

Table 6.1: Thermodynamic Properties of Compression Refrigeration Cycle Points (at 2463 RPM and 20^{o}C Evaporator Temperature).

Points	Enthalpy (kJ/kg)	Pressure (kPa)	Entropy (kJ/kg.K)	Temperature (^{o}C)
[1]	267.1	572.1	0.9409	25,55
[2]	318.6	2166	1,005	99.01
[3]	150	2166	0.5195	66.56
[4]	150	572.1	0.5417	20

Additionally, the other important parameters using in Matlab code, are obtained from EES such as the mass flow rate, COP and refrigerant outlet quality. Their values are given in Table 6.2.

Table 6.2: Results of Additional Thermodynamic Properties (at 2463 RPM and 20^{o}C Evaporator Temperature)

Mass Flow Rate	0.003075 kg/s
COP	1.661
Inlet Quality	x[4]= 0.39

From the data in Figure 6.1 and Figure 6.2, the relation between the varying thermodynamic properties can be shown as a diagram.

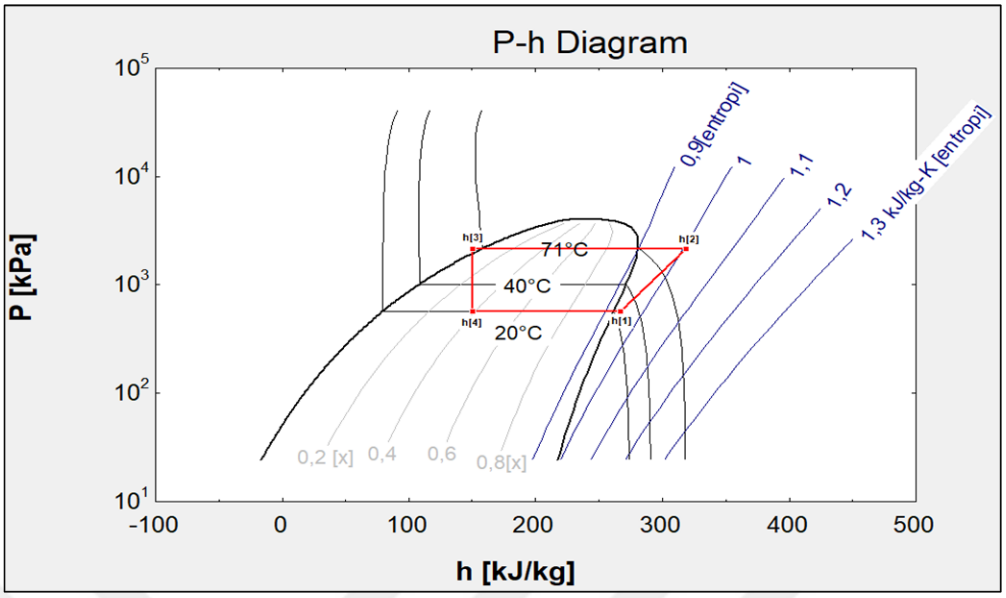

Figure 6.1: P-h Diagram (at 2463 RPM and 20°C Evaporator Temperature).

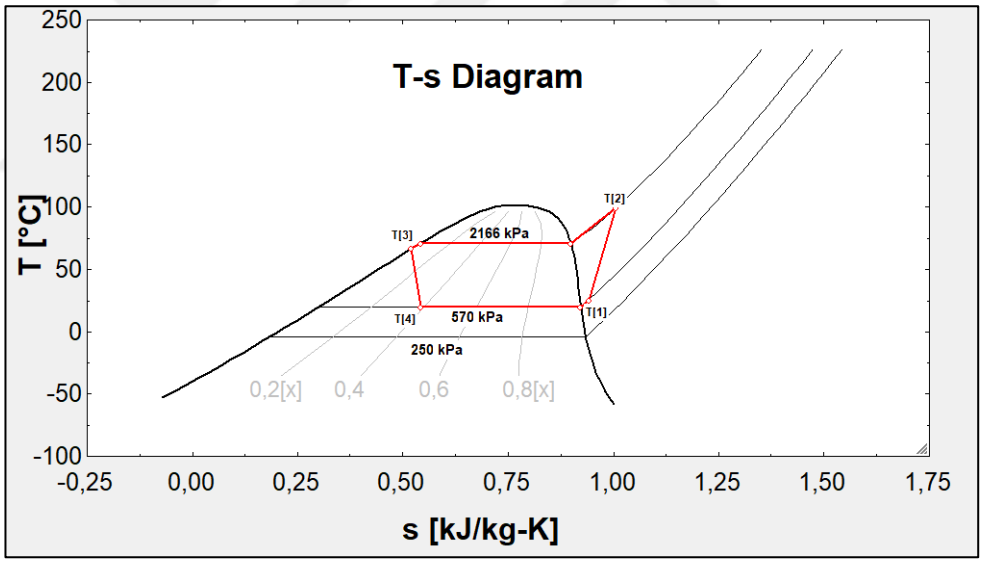

Figure 6.2: T-s Diagram (at 2463 RPM and 20°C Evaporator Temperature).

Alternatively, the thermodynamic properties are investigated with the evaporator temperature of 10°C and the rotational speed of 4238 RPM. Calculation results are found and shown in Table 6.3.

Table 6.3: Thermodynamic Properties of Compression Refrigeration Cycle Points (at 4238 RPM and 10°C Evaporator Temperature).

Points	Enthalpy (kJ/kg)	Pressure (kPa)	Entropy (kJ/kg.K)	Temperature (°C)
[1]	261.4	414.9	0,9446	15,55
[2]	333.7	2166	1.045	111.5
[3]	150	2166	0.5195	66.56
[4]	150	414.9	0.5515	10

After the calculation, additional data is collected due to thermodynamic properties from previous table. The comparison indicates that mass flow rate and quality parameters at evaporator temperature of 10°C is higher than the first results. On the contrary, COP value decreases for this condition. The values are given in Table 6.4.

Table 6.4: Results of Additional Thermodynamic Properties (at 4238 RPM and 10°C Evaporator Temperature).

Mass Flow Rate	0.003232 kg/s
COP	1.54
Inlet Quality	x[4]= 0.44

Finally, thermodynamic diagrams of this cycle are generated, and they can be seen from Figure 6.3 and Figure 6.4.

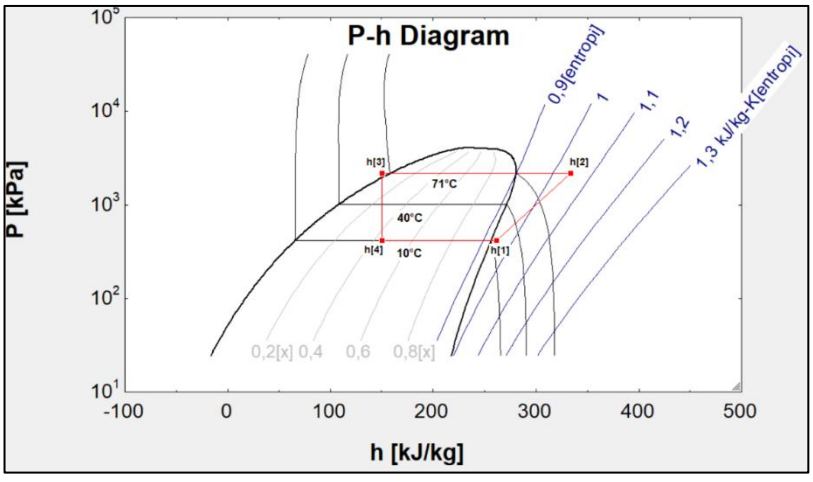

Figure 6.3: P-h Diagram (at 4238 RPM and 10°C Evaporator Temperature).

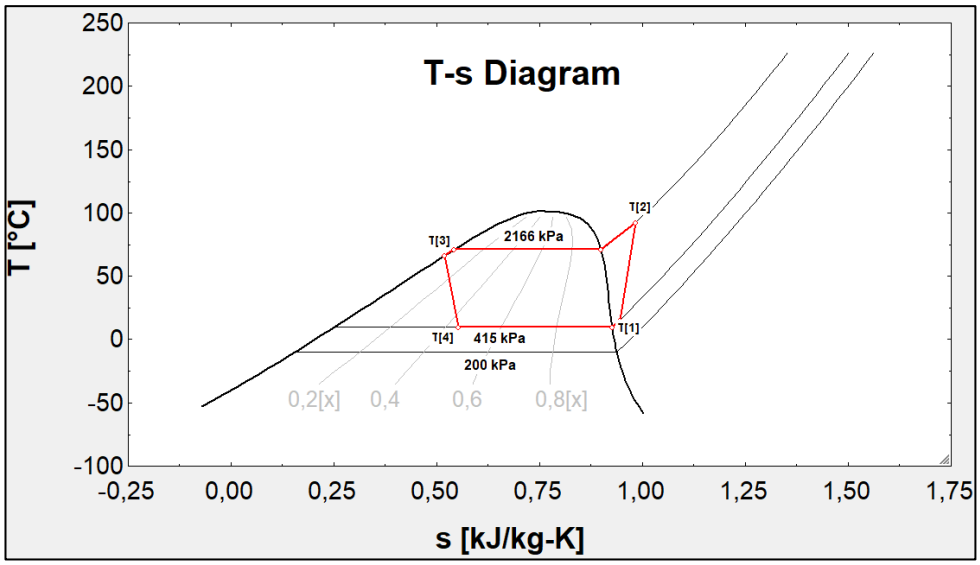

Figure 6.4: T-s Diagram (at 4238 RPM and 10^{o}C Evaporator Temperature).

6.2. Parametric Analysis

Evaporator dimensions can be determined by the corresponding pressure drop and heat transfer coefficient, which can be approximated by single and two-phase flow equations.

6.2.1. Heat Transfer Coefficient

The first findings in Matlab are about the relation among heat transfer coefficient, length and evaporator temperature. It is mentioned previous chapters; three different parameters can be obtained from this analysis. Two-phase and single-phase heat transfer coefficients occur naturally while heat transfer correlation is derived from other coefficients. Thus, the singularity issue that occurs due to equations 3.18 and 3.19 can be prevented. In these diagrams, purple curve describes the heat transfer correlation, red curve is also two-phase heat transfer coefficient. Last one, blue, is defined as single-phase heat transfer.

The relation between heat transfer coefficient and length is demonstrated in Figure 6.5 when evaporator temperature is fixed at 20^{o}C. It is observed that the heat transfer coefficient decreases as the pipe length increases. According to pipe length,

initial value of two-phase heat transfer coefficient changes from 50.000 to 45.000 W/m^2K.

All the results of heat transfer coefficients are demonstrated in Table 6.5.

Table 6.5: Results of Heat Transfer Coefficients (Two and Single-phase).

Evaporator Temperature	Length	Two-Phase Heat Transfer Coefficient Distributions	Single-Phase Heat Transfer Coefficient Distributions
10°C	1 m	16499-389.52	182.17-351
	3 m	14153.0-334.14	182.17-351
	5 m	13544.23-319.76	182.17-351
20 °C	1 m	17158.1-430	165.58-344.54
	3 m	13106.0-329.21	164.58-344.54
	5 m	12054-302.78	165.58-344.54

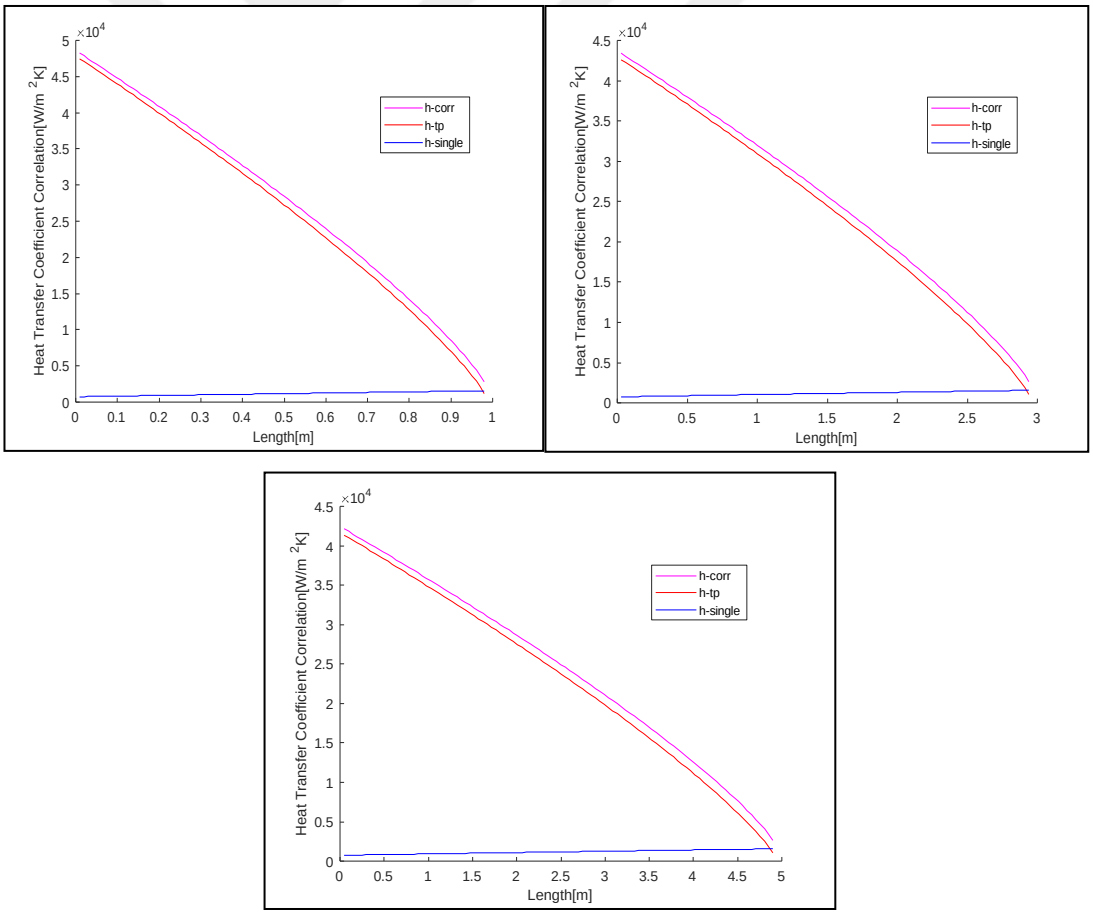

Figure 6.5: Heat Transfer Coefficient Distribution (at 20°C Evaporator Temperature with the channel lengths 1,3 and 5 meters).

When the evaporator temperature is reduced to 10°C, heat transfer coefficient shows the same behavior along the evaporator channel. However, the results of two-phase heat transfer coefficient values are more than the first case. Initial two-phase heat transfer coefficient can reach up to 60.000 W/m^{2}K. The heat transfer coefficients at 10 °C of evaporator temperature are shown in Figure 6.6.

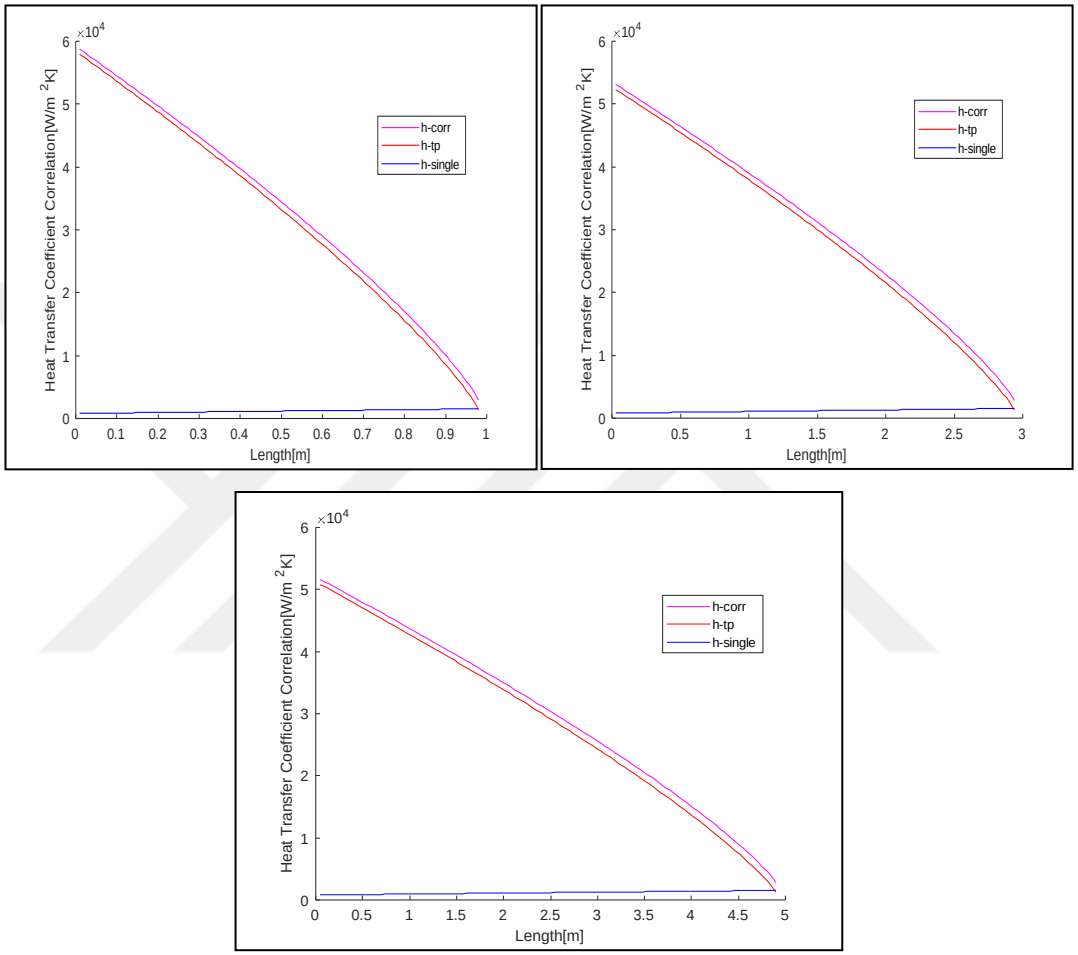

Figure 6.6: Heat Transfer Coefficient Distribution (at 10°C Evaporator Temperature with the channel lengths 1,3 and 5 meters).

6.2.2. Pressure Drops

Pressure drops approach is similar to heat transfer approaches that can be varied due to evaporating temperature. The results present the different types of pressure drop that is considered in this study. Equations 3.9, 3.10 and 3.11 include the data of two-phase region while equation 3.28 provide information about single-phase pressure drops.

Types of pressure drops are investigated by changing the length at constant evaporating temperature of 20°C. As it can be seen from Figure 6.7, total pressure drop dramatically increases when the length is extended.

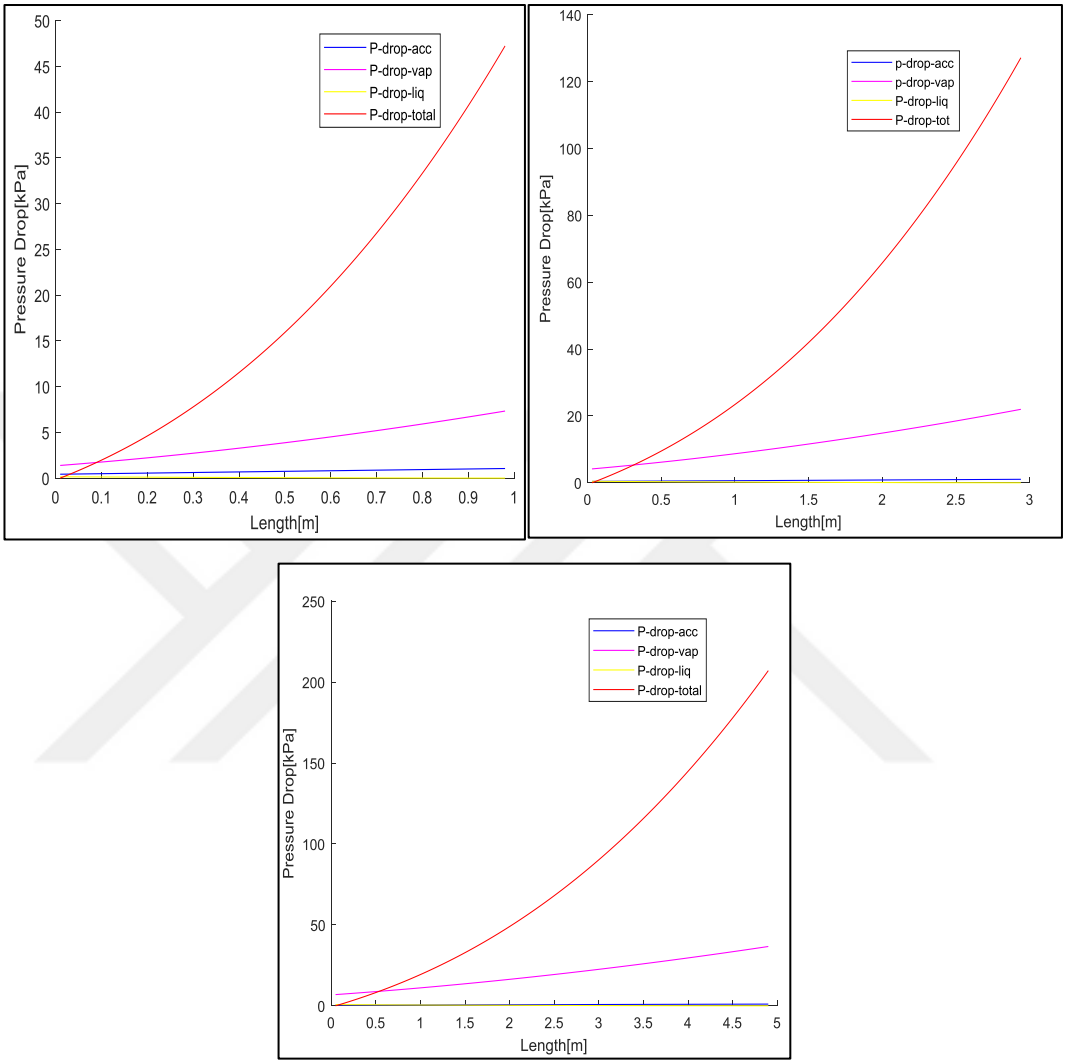

Figure 6.7: Pressure Drops (Acceleration, Vapor, Liquid, Total at evaporating temperature of 20°C with the channel lengths 1,3 and 5 meters).

In second case described as working at 10°C of evaporator temperature, pressure drops can reach higher levels than first case. Total pressure drop reaches up to between 275 and 325 kPa. Therefore, the pipe length should be considered as a constituent part of pressure drop calculation. Figure 6.8 give the changes on along the pipe length.

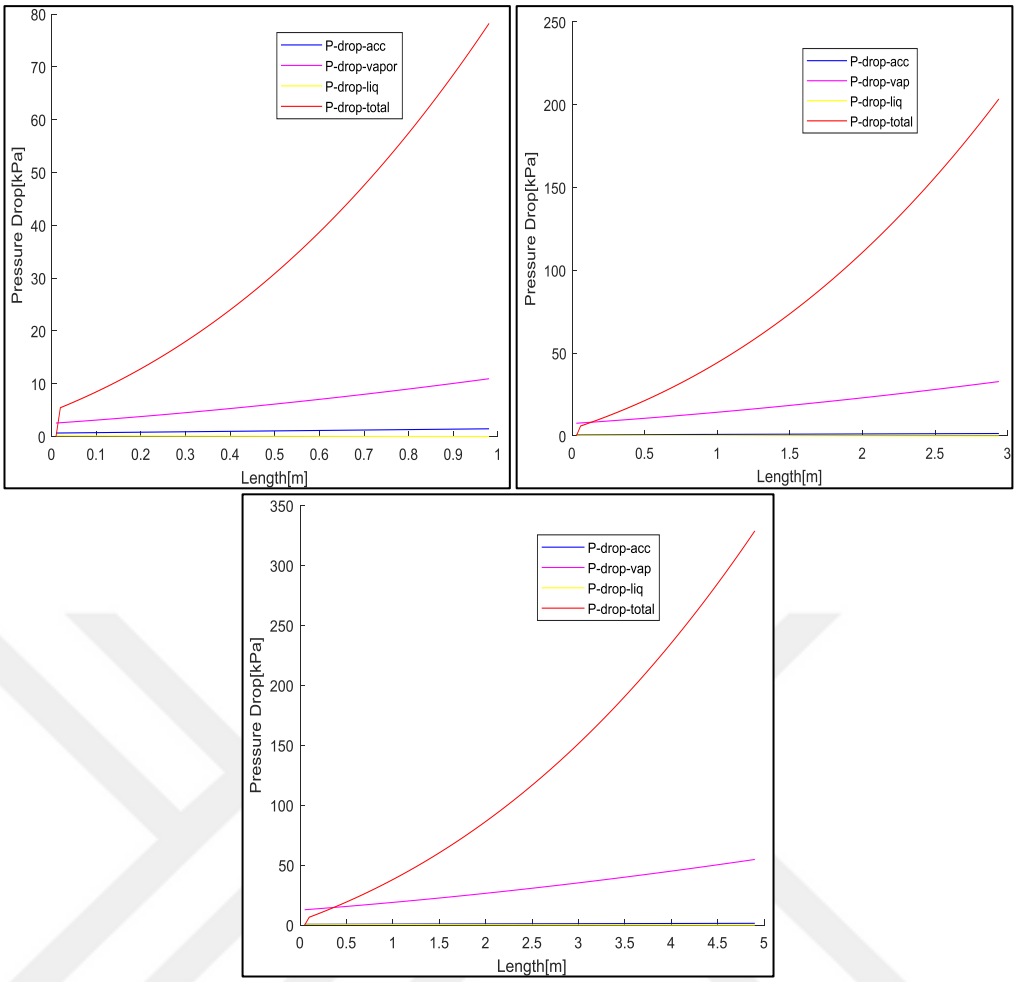

Figure 6.8: Pressure Drops- (Acceleration, Vapor, Liquid, Total at evaporating temperature of 10^{o}C with the channel lengths 1,3 and 5 meter).

6.2.3. Wall Temperature Distribution

In this calculation, changing of temperature values of side wall, along the evaporator channel and refrigerant in the evaporator are investigated the course of the cooling process. In this analysis, side wall, channel wall and refrigerant temperatures are examined for being a particular synergy. Final point of findings tends to go to the infinity because of the uncertainty on the heat transfer coefficient correlation.

The side wall temperature and refrigerant temperature are symbolized as T_s and T_m respectively. T1 is also called as the temperature of the copper evaporator channel. In these figures, T1 is indicated by the red curve and T_s by the blue curve. Similarly, refrigerant temperature in the evaporator represented as purple points.

At 20°C of refrigerant temperature, T_s increases from 20 °C to 120 °C. In the same direction, T1 changes range from 15 °C to 50 °C, however the length of channel increases 1 to 5 meters, the optimum point of temperature values constantly decreases and continues to decrease to the refrigerant temperature level. Figure 6.9 shows the relationship between temperature distribution and the length of evaporator channel with respect to 1, 3 and 5 meters.

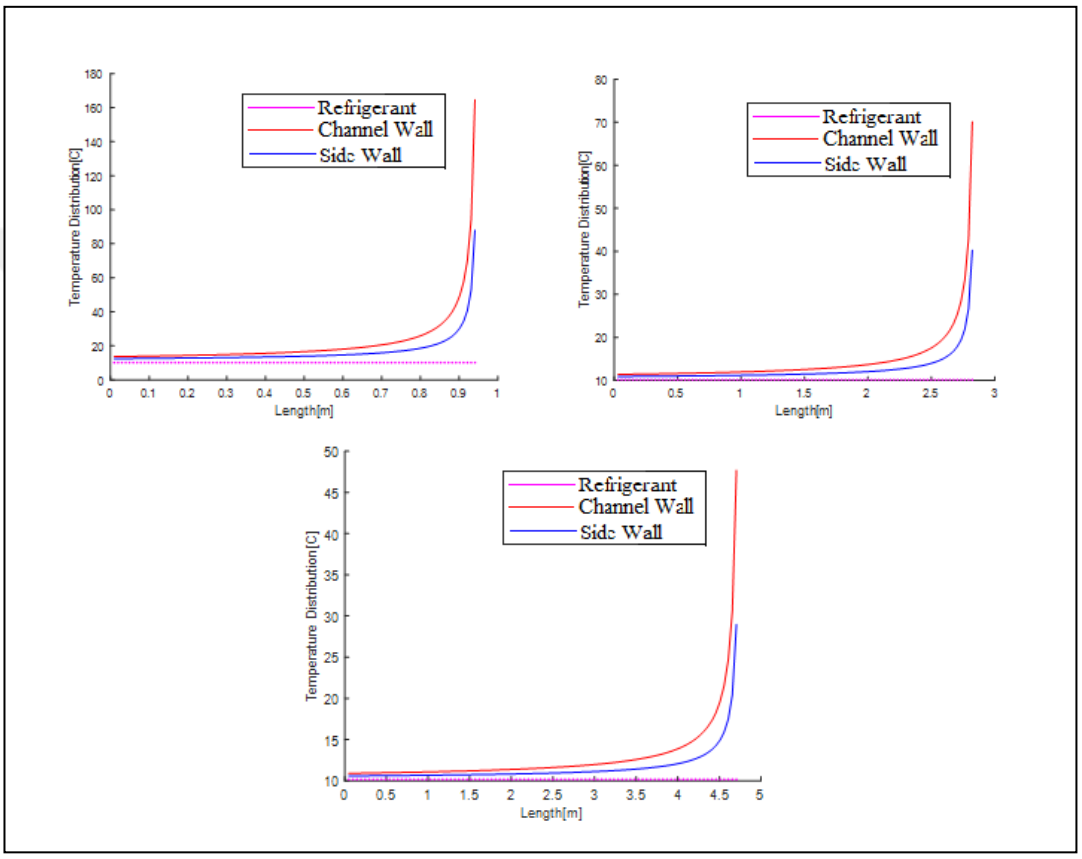

Figure 6.9: Temperature Distribution for Refrigerant, Side Wall and Channel Wall (at evaporator temperature of 20°C with the channel lengths 1,3 and 5 meter).

The same temperature distributions along the selected parts occur at evaporator temperature of 10 °C. Addition to first case, the range of wall temperature values are varying from 10 °C to 170 °C and channel wall temperature reaches up to 80 °C. All temperature distributions at 10 °C are presented in Figure 6.10.

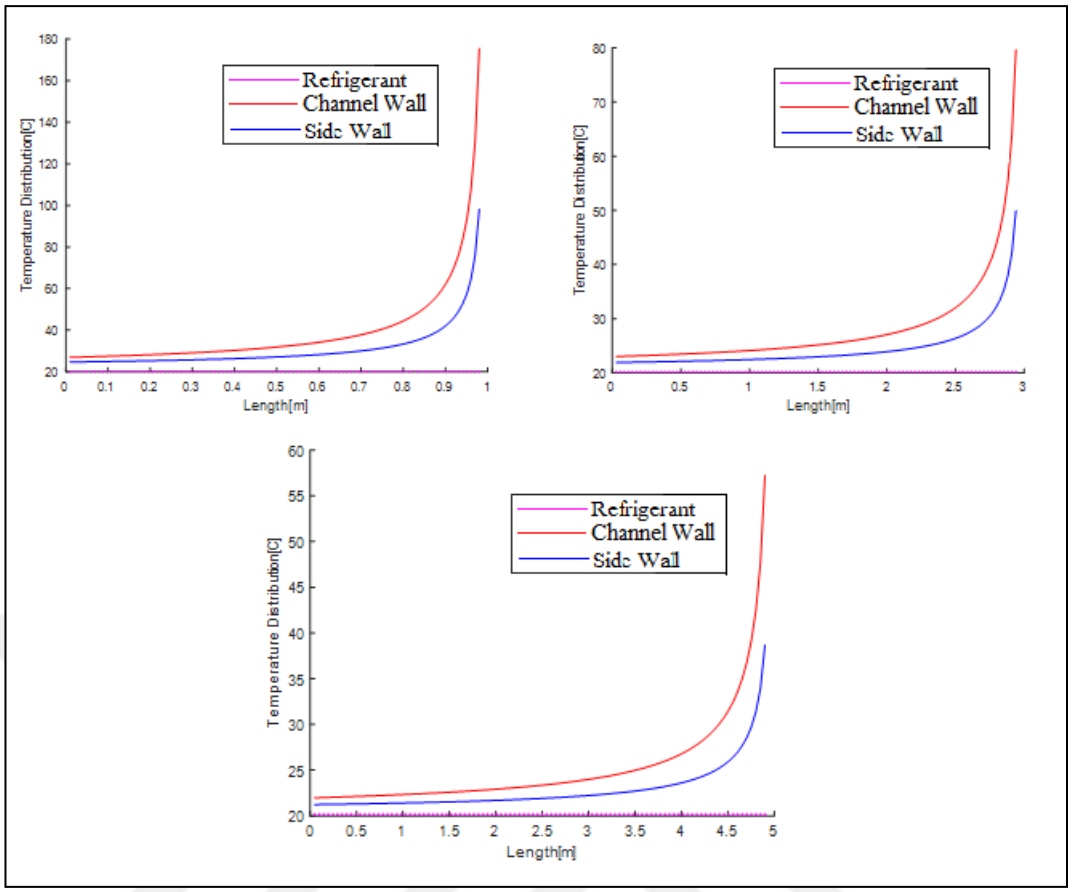

Figure 6.10: Temperature Distribution for Refrigerant, Side Wall and Channel Wall (at evaporator temperature of 10^{o}C with the channel lengths 1,3 and 5 meter).

6.3. Experimental Analysis

Experimental analyses on test bench are investigated in three different cases.

6.3.1. At Room Temperature (24 ^{o}C)

In this study, the ambient temperature is constant, however the thermal load of system is controlled by host-computer. Thus, this cooling system can be separately operated at full or both full and half thermal loads.

Thermal camera is also used for this application. Because, the images from the thermal camera shows the temperature distribution on the condenser under different conditions which are described in previous section. The same operations can be used for evaporators.

For transient state and full thermal load analysis, the fan is operated at 15 percent of its capacity and also the compressor is worked at low speed. The condenser temperature varies from 43.3 ^{o}C to 23.8 ^{o}C, while evaporator temperatures change from 47 ^{o}C to 20.7 ^{o}C at full thermal load.

Figure 6.11: Condenser Temperature Distribution at Full Load.

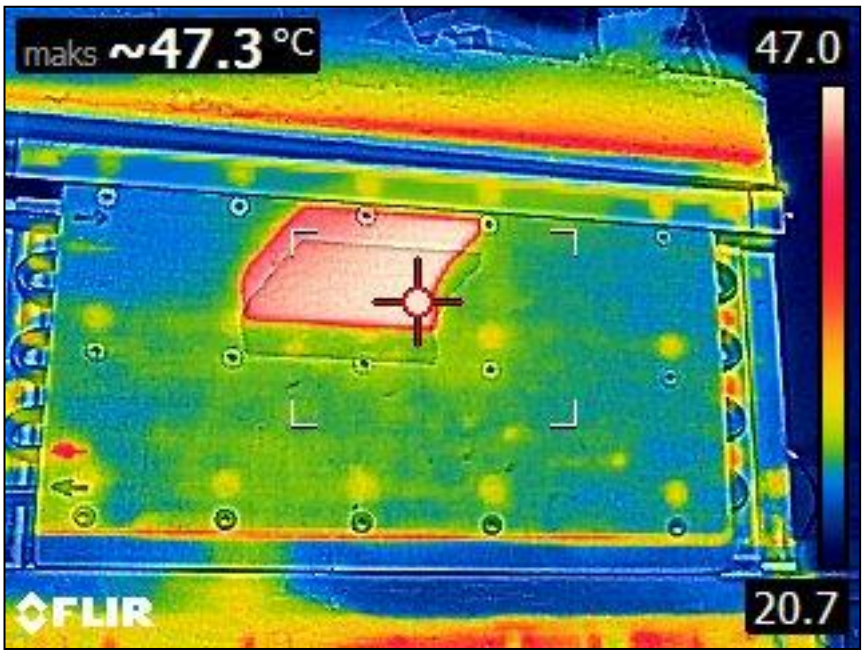

Figure 6.12: Evaporator Temperature Distribution at Full Load.

The temperature values obtained from sensors are plotted as a function of time in Figure 6.13. TS3, TS5, TS6 and TS7 are located to the computer side wall respectively. The unit of x axis is a second and the unit of y axis is a Celsius.

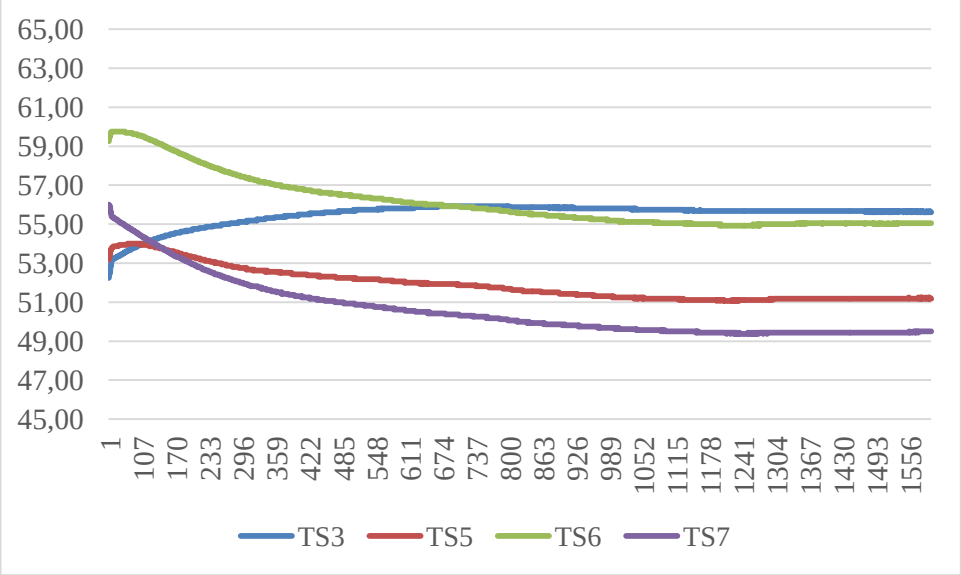

Figure 6.13: Temperature Distributions on Side Walls at Full Load Capacity (Temperature-^{o}C and Time-sec).

Second case has fulfilled under the same conditions. Operating at full thermal load affects the change of condenser temperature from 43.6^{o}C to 23.4^{o}C, also the change of evaporator temperature from 58.2^{o}C to 15.5^{o}C.

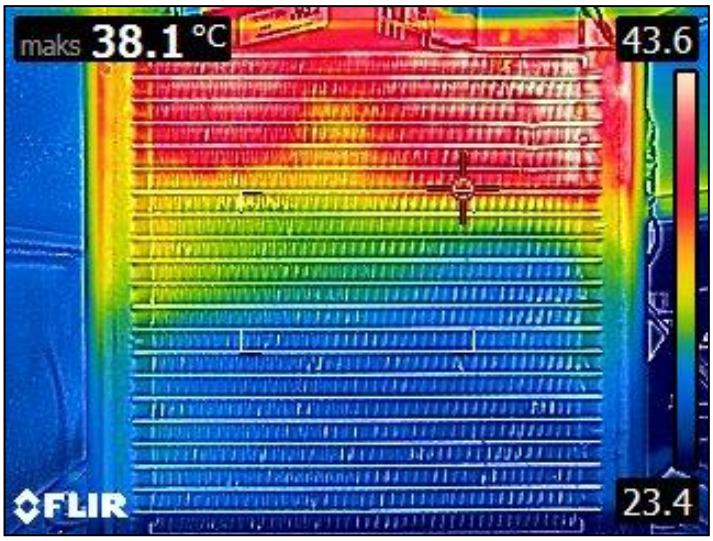

Figure 6.14: Condenser Temperature Distribution at Full Load.

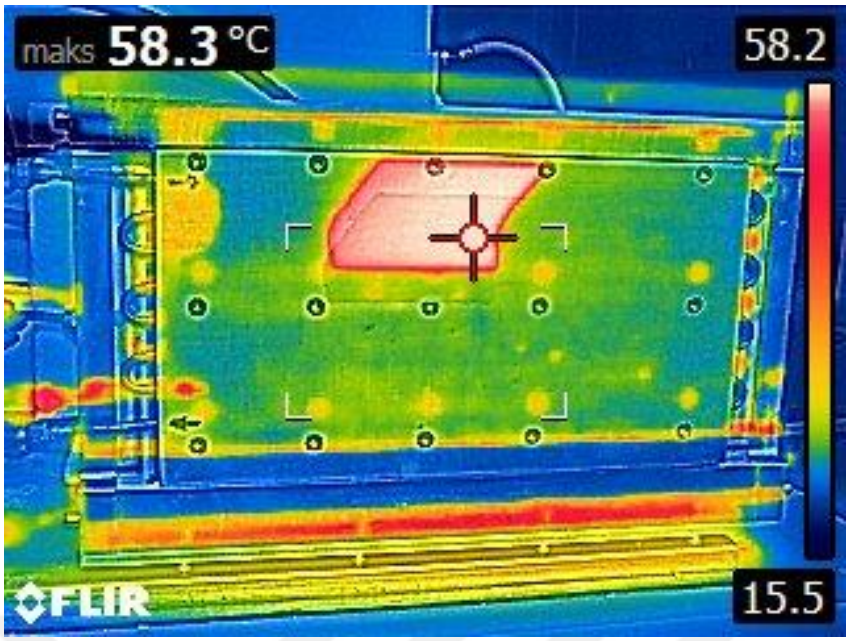

Figure 6.15: Evaporator Temperature Distribution at Full Load.

After applying the half thermal load to the system, condenser temperature has changed between 43.8 and 23.5 ^{o}C.

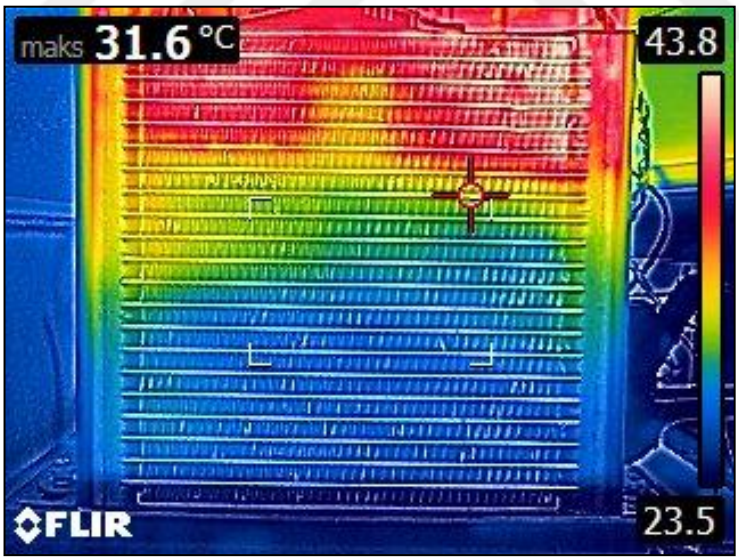

Figure 6.16: Condenser Temperature Distribution at Half Load.

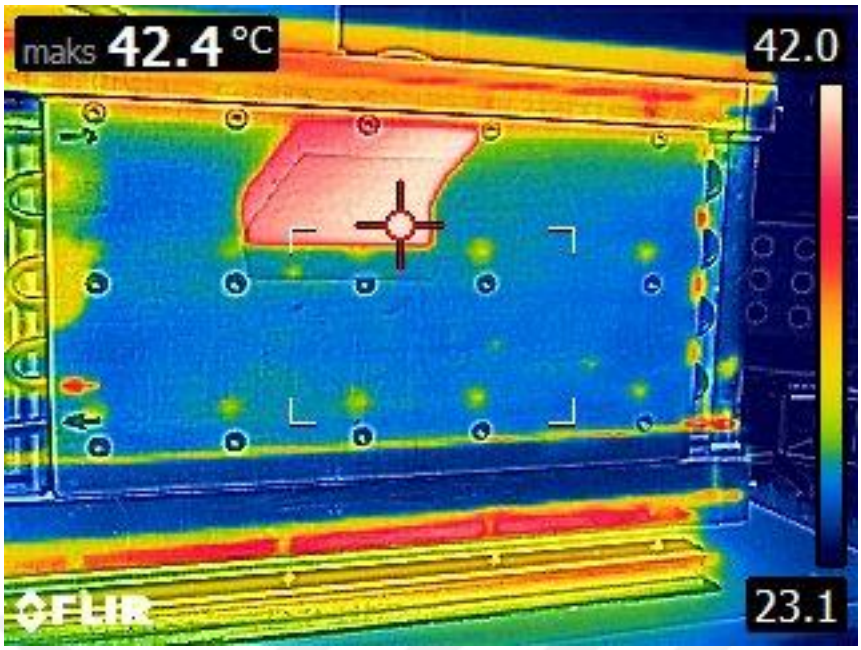

Figure 6.17: Evaporator Temperature Distribution at Half Load.

The temperature values obtained from side wall sensors (TS3, TS5, TS6 and TS7) are plotted as a function of time in Figure 6.18. Full and half load conditions are operated within fixed times steps alternately until the system reaches to the periodic behavior. The unit of x axis is a second and the unit of y axis is a Celsius.

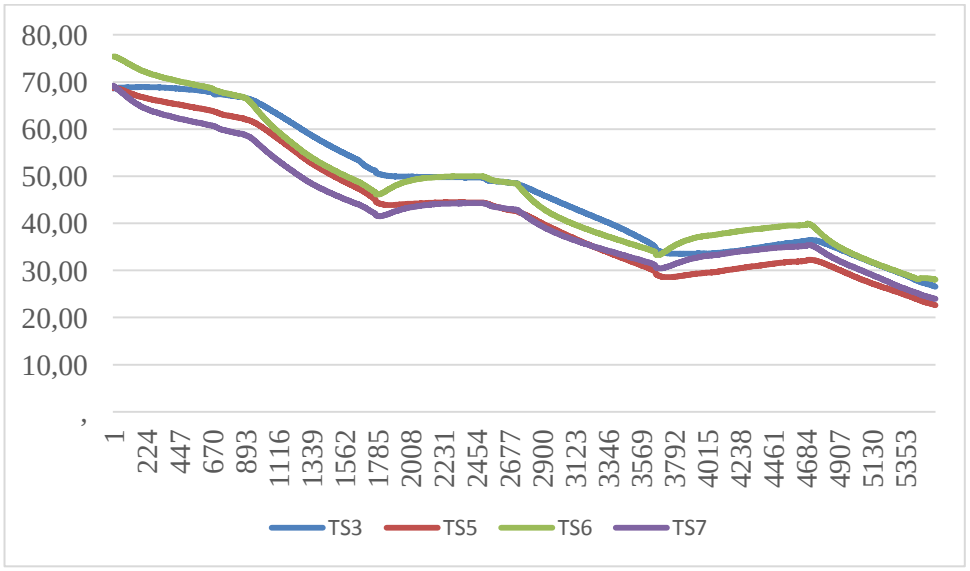

Figure 6.18: Temperature Distributions on Side Walls at Both Full and Half Load Capacity (Temperature-^{o}C and Time-sec).

6.3.2. At 40 °C of Ambient Temperature

The temperature distributions on the condenser and evaporators at half thermal load according to the transient state can be seen from Figure 6.17 and 6.18 respectively.

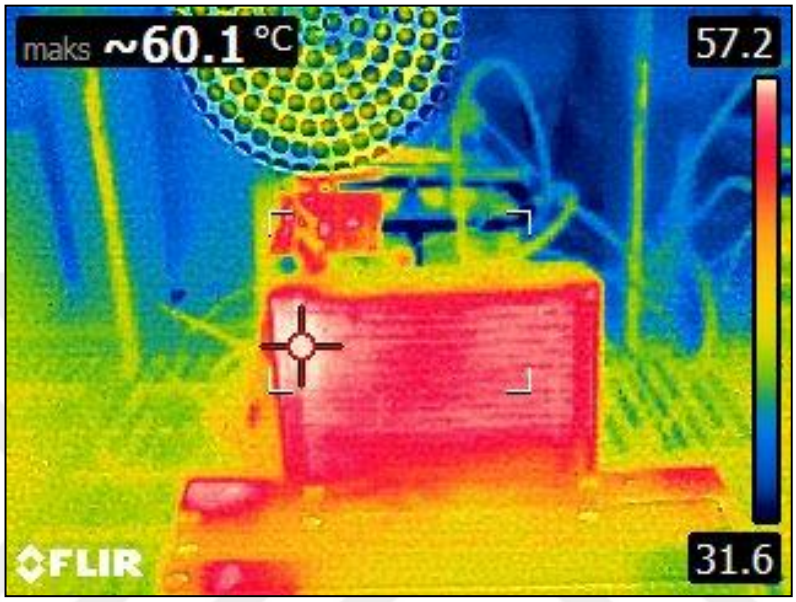

Figure 6.19: Condenser Temperature Distribution at Half Load.

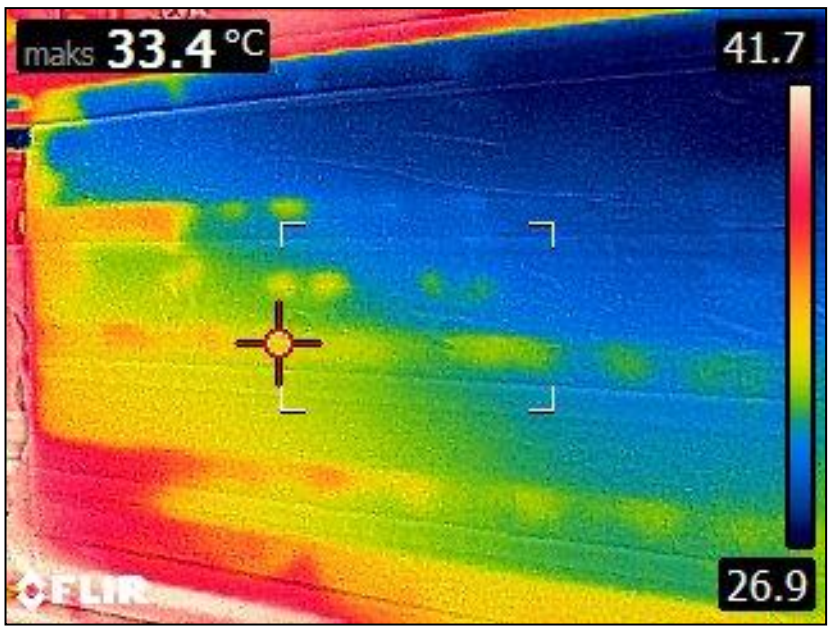

Figure 6.20: Evaporator Temperature Distribution at Half Load.

The temperature values from side wall sensors at 44 ^{o}C of ambient temperature working with fan at 20 percent of capacity and compressor at 40 percent of capacity can be seen as below. The unit of x axis is second and the unit of y axis is Celsius.

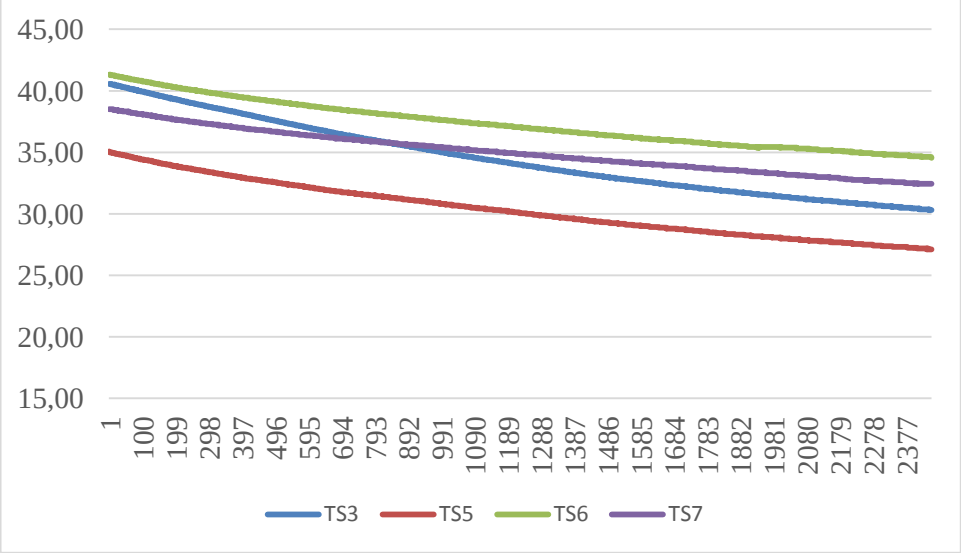

Figure 6.21: Temperature Distributions on Side Walls at Half Load Capacity(Temperature-^{o}C and Time-sec).

The same operations are conducted at full thermal load under the transient conditions. These findings for the condenser are demonstrated in Figure 6.22. The condenser temperature changes from 58.2^{o}C to 31.7 at full thermal load.

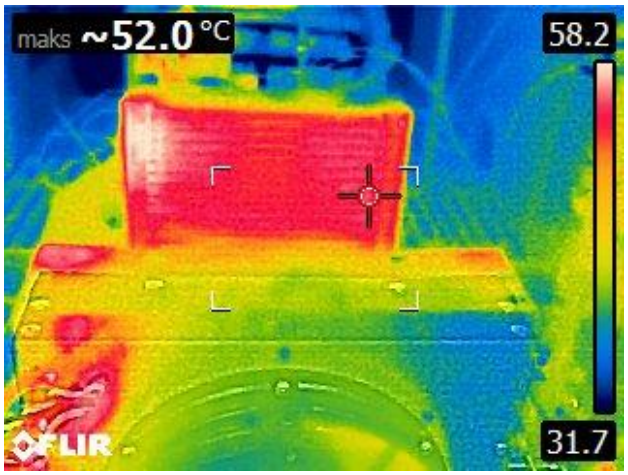

Figure 6.22: Condenser Temperature Distribution at Full Load.

The temperature values for selected locations of cooling cycle are plotted in Figure 6.23. The fan and compressor operating capacities are increased during the study. Fan is operated from 25 to 40% while compressor is working at 40 to 55%. Side wall temperature is increased up to 50 ^{o}C while the cooling system is working. Therefore, it can be seen that compressor and fan cannot affect the wall temperature when they are operated at low speed capacity.

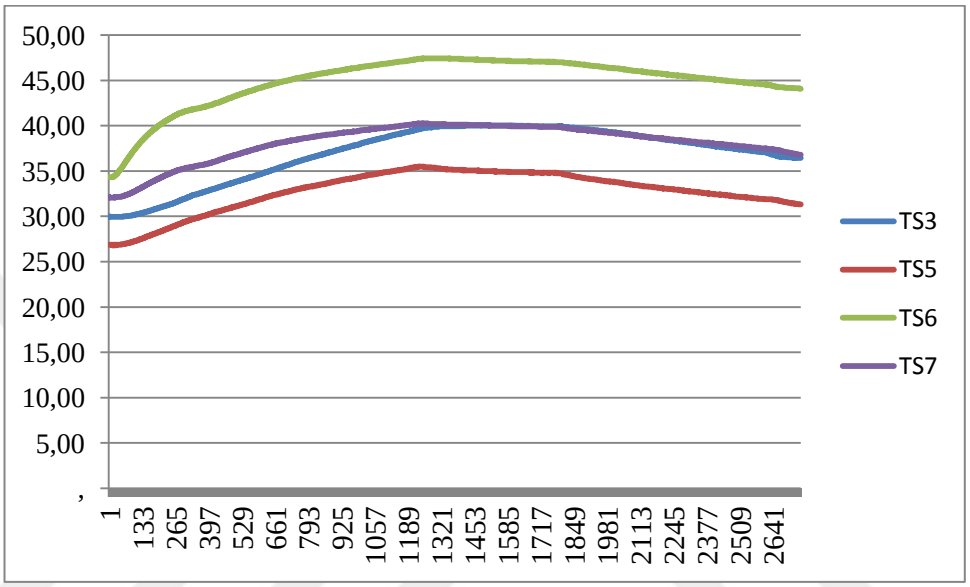

Figure 6.23: Temperature Distributions on Side Walls at Both Full and Half Load Capacity.

7. CONCLUSION & FUTURE WORKS

In this paper, a novel refrigeration system is enabled by a selected miniature compressor and micro-channel based condenser and evaporators. This refrigeration system is designed by the helps of Engineering Equation Solver, Matlab and experimental analysis. Working conditions and limitations are determined based on the study objectives to make a compressor and refrigerant selection, then their properties lead to the study for next steps.

Operating conditions are transmitted to Engineering Equation Solver and they are applied with the vapor compression refrigeration cycle equations in order to obtain the thermodynamic properties of cycle points such as enthalpy, pressure, mass flow rate etc. To make a comparison and create an alternative case, the thermodynamic properties have been investigated at 10 ^{o}C and 20 ^{o}C of evaporator temperature with the help of compressor cooling capacity and compressor input power diagrams.

Using the Matlab program enables to determine and design evaporator according to heat transfer coefficient and pressure drop parameters. These parameters are calculated by considering the flow regimes, phase types and length and dimension of evaporator channel. Flow regimes can change and affect the temperature distribution of side walls and evaporator channels depending on heat transfer coefficients. Heat transfer coefficient studies in evaporator indicates that two phase and single-phase flow occur along the evaporator channels. Hence, heat transfer coefficients can be calculated relating with these phase equations. The same mathematical approach applies to the pressure drop calculation. Similarly, this thesis has provided a deeper insight into the significance of evaporator channel length.

Additionally, the rest of refrigeration system components such as expansion valve, condenser etc. is selected as a result of mathematical calculation. In order to build a test bench, all of cooling components and computer cabin are integrated according to pipe and instrumentation diagram. Management system of test bench is also developed to obtain the temperature and pressure values from tests.

Future works need to be done to develop this system. For the purpose of developing this system, the compressor must be produced to reduce foreign dependency. Next studies on this project must be based on obtaining higher COP

value from EES, similarly consider the effects of bend numbers and bend pressure drops for the evaporator design in Matlab.

Alternative expansion valves, especially electronic types, should be tried and finally, additional performance tests need to be conducted improving this system.

REFERENCES

[1] Moran M. J. and Shapiro H. N., (2010), Fundamentals of Engineering Thermodynamics, Seventh Edition, Wiley.

[2] Cengel Y. and Boles M. A., (2013), "Thermodynamics An Engineering Approach," Fourth Edition, Mc Graw Hill.

[3] Heydari A. (2002), "Miniature vapor compression refrigeration systems for active cooling of high performance computers," Intersoc. Conf. Therm. Thermomechanical Phenom. Electron. Syst. ITHERM, 371–378, San Diego, California, USA (May 30-June 1, 2002).

[4] Chang C. C. , Liang N. W., and Chen S. L. , (2010) "Miniature vapor compressor refrigeration system for electronic cooling," IEEE Trans. Components Packag. Technol., vol. 33, no. 4, pp. 794–800.

[5] Yildiz S., (2010) "Design and Simulation of a Vapor Compression Refrigeration Cycle for a Micro Refrigerator," The Degree of Master of Science, Middle East Technical University

[6] Trutassanawin S., Groll E. A., Garimella S. V., Cremaschi L. (2006), "Experimental investigation of a miniature-scale refrigeration system for electronics cooling," IEEE Trans. Components Packag. Technol., 29 (3), 678–687.

[7] Mongia R. et al., (2006) "Small scale refrigeration system for electronics cooling within a notebook computer," in Thermomechanical Phenomena in Electronic Systems -Proceedings of the Intersociety Conference, San Diego, CA, USA, (30 May - 02 June 2006).

[8] Mehendale S. S., Jacobi A. M., and Shah R. K., (2009) "Fluid Flow and Heat Transfer at Micro- and Meso-Scales With Application to Heat Exchanger Design," Appl. Mech. Rev, Vol. 53, 175-193 .

[9] Ide H., Kariyasaki A., and Fukano T., (2006) "Fundamental data on the gas–

liquid two-phase flow in minichannels," Int. J. Therm. Sci., Vol 46, Pages: 519-530.

[10] Hsieh Y. Y. and Lin T. F., (2002) "Saturated flow boiling heat transfer and pressure drop of refrigerant R-410A in a vertical plate heat exchanger," Int. J. Heat Mass Transf., Vol. 45, Pages 1033-1044.

[11] Lazarek G. M. and Black S. H., (1982) "Evaporative heat transfer, pressure drop and critical heat flux in a small vertical tube with R-113," Int. J. Heat Mass Transf., Vol. 25, Pages 945-960.

[12] Kandlikar S. G. and Steinke M. E., (2003) "Predicting heat transfer during flow boiling in minichannels and microchannels," in ASHRAE Transactions 109:667-676.

[13] Signal D. L., Sham D. R., and Kumar S., (2015), "Single and Two Phase Pressure Drop in Fluid Flow," Int. J. Latest Trends Eng. Technol., vol. 6, no. 2, pp. 28–33.

[14] Sathe A. A., Groll E. A., and Garimella S. V, (2008) "Experimental evaluation of a miniature rotary compressor for application in electronics cooling," ICECP, Int. Compress. Eng. Conf. 19, 1115- Page:1-12, Purdue USA, (July 14-17, 2008)

[15] Coskun F., (2019) "Vapor Compression Refrigeration Cycle Design for Electronic Cooling Applications," The Degree of Master of Science, Gebze Technical University.

[16] Web 1, (2015), https://www.aspencompressor.com, (Erişim Tarihi 18/11/2018).

[17] Fischer S.K., Rice C.K., (1983) "The Oak Ridge Heat Pump Models: I. A Steady-State Computer Design Model of Air-to-Air Heat Pumps," Oak Ride National Library, Report Number: ORNL/CON-80/R1.

[18] Shah R. K. and Sekulic D. P. (2003), Fundamentals of Heat Exchangers, First

Edition, Wiley.

[19] Kakaç S., Shah R. K., (1987) "Handbook of Single-Phase Convective Heat Transfer" First Edition, Wiley-Interscience.

[20] Web 2, (2016), https://www.swep.net/refrigerant-handbook/4.-expansion-valves/adf6/, (Erişim Tarihi 20/12/2018).

[21] Flannery M. D., Schmidt J, and Thorson K., (2016) "Thermal Enhancements for Separable Thermal Mechanical Interfaces," in 46th AIAA Thermophysics Conference, Washington D.C, USA (June 13-17, 2016).

BIOGRAPHY

Salih Can Dönmez was born in İstanbul in 1994. He graduated from İstanbul University with a bachelor's degree in 2016 and he became a mechanical engineer. Then he applied to Gebze Technical University in 2017. Now, he continues his career as a master student in the department of Energy Systems in Mechanical Engineering of Gebze Technical University, Graduate School of Natural and Applied Sciences.